Universiteit
Leiden
The Netherlands

From stem cells to functional lymphocytes: cell differentiation and gene therapy implementation for RAG-SCID

García Pérez, L.

Citation
García Pérez, L. (2021, October 6). *From stem cells to functional lymphocytes: cell differentiation and gene therapy implementation for RAG-SCID*. Retrieved from https://hdl.handle.net/1887/3214836

Version:	Publisher's Version
License:	Licence agreement concerning inclusion of doctoral thesis in the Institutional Repository of the University of Leiden
Downloaded from:	https://hdl.handle.net/1887/3214836

Note: To cite this publication please use the final published version (if applicable).

Chapter 4

Successful preclinical development of gene therapy for Recombinase Activating Gene-1-deficient SCID

Laura Garcia-Perez[1], Marja van Eggermond[1], Lieke van Roon[1], Sandra Vloemans[1], Martijn Cordes[1], Axel Schambach[2], Michael Rothe[2], Dagmar Berghuis[3], Chantal Lagresle-Peyrou[4], Marina Cavazzana[4], Fang Zhang[5], Adrian J. Thrasher[5], Daniela Salvatori[6-9], Pauline Meij[7], Anna Villa[8], Jacques J.M. Van Dongen[1], Jaap-Jan Zwaginga[1], Mirjam van der Burg[3], H Bobby Gaspar[5], Arjan Lankester[3], Frank J.T. Staal[1]*, Karin Pike-Overzet[1].

[1.] Department of Immunohematology and Blood Transfusion, Leiden University Medical Center, The Netherlands.
[2.] Institute of Experimental Hematology, Hannover Medical School, Germany.
[3.] Willem-Alexander Children's Hospital Department of Pediatrics, Leiden University Medical Center, The Netherlands.
[4.] Biotherapy Clinical Investigation Center, Groupe Hospitalier Universitaire Ouest, Assistance Publique-Hôpitaux de Paris, INSERM CIC 1416, Paris, France. Laboratory of Human Lymphohematopoiesis, INSERM UMR 1163, Imagine Institute and Paris Descartes University – Sorbonne Paris Cité, France And Department of Biotherapy, Necker Children's Hospital, Assistance Publique-Hôpitaux de Paris, France.
[5.] Molecular and Cellular Immunology, Great Ormond Street Institute of Child Health, and Great Ormond Street Hospital NHS Trust, UK.
[6.] Central Laboratory Animal Facility, Pathology Unit, Leiden University Medical Center, The Netherlands.
[7.] Department of Pharmacy, Leiden University Medical Center, The Netherlands.
[8.] Pathogenesis and treatment of immune and bone diseases Unit, San Raffaele, Telethon Institute for Gene Therapy (SR-Tiget), IRCCS San Raffaele Scientific Institute, Italy
[9.] Anatomy and Physiology Division, Clinical Sciences, Faculty of Veterinary Medicine, Utrecht University, The Netherlands

Molecular Therapy: Methods&Clinical Development,2020,Vol.17,666

ABSTRACT

Recombinase-activating gene-1 (RAG1) deficient SCID patients lack B and T lymphocytes due to the inability to rearrange immunoglobulin and T-cell receptor genes. Gene therapy is an alternative for those RAG1-SCID patients who lack a suitable bone marrow donor. We designed lentiviral vectors with different internal promoters driving codon optimized RAG1 to ensure optimal expression. We used Rag1-/- mice as preclinical model for RAG1-SCID to assess the efficacy of the various vectors. We observed that B- and T-cell reconstitution directly correlated with RAG1 expression. Mice with low RAG1 expression showed poor immune reconstitution; however higher expression resulted in phenotypic and functional lymphocyte reconstitution comparable to mice receiving wild type stem cells. No signs of genotoxicity were found. Additionally, RAG1-SCID patient CD34+ cells transduced with our clinical RAG1 vector and transplanted into NSG mice led to improved human B- and T-cell development. Together with favorable safety data, these results substantiate a clinical trial for RAG1-SCID.

INTRODUCTION

Severe combined immunodeficiency (SCID) is a life-threatening disorder of the adaptive immune system [1]. In all forms of SCID, the development of T cells in the thymus is arrested due to genetic defects in genes essential for this complex process, while concomitant deficiencies in B lymphocytes and NK cells are depending on the SCID genotype. Affected infants are born with a severe T-lymphocyte deficiency and die within the first year of life unless effective treatment is given. Curative treatment options are limited and confined to allogeneic hematopoietic stem cell transplantation [2, 3] and autologous stem cell gene therapy [4, 5].

Over 20 different genes have been shown to be causative for SCID[1]. Three major types of SCID exist, the common gamma chain cytokine deficiencies, mainly due to defects in the Il2Rγ chain (which is also termed the common γ-chain). The JAK3 and Il7Ra deficiency are much more rare but also fall into this category. The second type of SCID concerns metabolic enzymes that affect highly proliferating cells such as immature thymocytes. Adenosine deaminase (ADA) deficiency is the prototype disease for this subtype, but other deficiencies have also been found, for instance PNP deficiency. The third major type of SCID is formed by recombination deficiencies. In these types of SCID the recombination machinery that is responsible for VDJ recombination of T-cell receptor (TCR) and Immunoglobulin (Ig) genes is affected. Examples are Recombination-activating gene 1 (RAG1), RAG2 deficiency and Artemis mutations. The exact nature of the T-cell developmental arrests in SCID patients has been difficult to elucidate because thymic biopsies cannot be taken, however recent functional experiments using bone marrow stem/progenitor cells from SCID patients has shown that most mutations lead to very early blocks in thymic differentiation [6-8].

Over the last 15 years, clinical trials of gene therapy for two major forms of SCID (SCID-X1 and ADA SCID) have shown significant safety and efficacy in correcting the immunodeficiency and allowing children to live normal functional lives [4, 5, 9-15]. This despite the occurrence of T-cell acute Lymphoblastic Leukemia (T-ALL) as a severe adverse effect in some of these early trials [16-19], which has led to an impetus to further develop safer vectors, the so-called self-inactivating (SIN) vectors [20-22].

For the recombination deficiencies, major steps have been made for correcting RAG1, RAG2 and Artemis deficiency. Artemis gene therapy is closest to clinical implementation and a first clinical trial has started in the US [23]. For RAG1-SCID several attempts to develop gene therapy have been made in the past, first with the now no longer acceptable γ-retroviral vectors [24], later with SIN lentiviral vectors [25, 26]. Our previous work reported successful restoration of Rag1 deficiency using SIN lentiviral vector technology and codon optimized RAG1 (c.o.RAG1) [26], however with a LV vector backbone that is not suitable for large scale GMP production and with a promoter that may lead to genotoxicity (see below). In this previous report, we obtained full restoration of peripheral T-cell numbers after 5 months using spleen focus-forming virus [SFFV]), approximately 35% of normal B-cell numbers, and importantly a polyclonal T-cell receptor (TCR) and B-cell receptor repertoire and full restoration of serum Ig levels, allowing functional responses after immunization with the T-cell–dependent antigens.

However, others have argued that using this approach, it is not possible to fully correct the RAG1 immune deficiency [27], and that oligoclonal T cells could develop, reminiscent of human Omenn syndrome, a disorder known to arise from hypomorphic RAG mutations, resulting in low recombinase activity. We have stated elsewhere [28] that these discrepant results can likely be explained by differences in the expression levels and low transduction efficiencies obtained for the therapeutic gene, *RAG1*. Here we report that successful restoration of the Rag1 deficiency can be obtained using SIN LV vectors that are clinically acceptable and importantly at low vector copy numbers (i.e., ~ 1 copy per cell).

A disadvantage of our previous lentiviral vectors was the use of the so-called RRL backbone, that gives relatively low titers in scaled-up virus productions needed for clinical application. Therefore, we switched to the CCL backbone that has been widely used clinically. In addition, the SFFV promoter sequence that was the most successful in our hands, has become less attractive due to assumed high risk of insertional mutagenesis [29]. Therefore we set out to develop a new set of SIN lentiviral vectors to express *c.o.RAG1* with different types of promoters and to test if they could correct Rag1 deficiency in a preclinical mouse model with low vector copy numbers, as to carry a lower risk of insertional mutagenesis. Through serendipitous effects in the viral production and titration of viral transduction, we obtained a whole range of *RAG1* expression *in vivo* ranging from very low to close to wild type levels. This allowed us to directly address the effects of differences in *RAG1* expression in a gene therapy setting. In addition, it has enabled us to choose a new SIN LV vector that functionally corrects the Rag1 deficiency *in vivo* in mice. The MND-c.o.RAG1 is now the vector of choice capable of high *RAG1* expression that is produced at clinical grade for an international multi-center RAG1-SCID gene therapy trial that is planned in the near future.

MATERIALS AND METHODS

Mice

57BL/6 Rag1$^{-/-}$ mice were originally obtained from The Jackson Laboratory (USA). C57BL/6 wild-type mice and NOD.Cg-Prkdc^{scid} Il2rg^{tm1Wjl}/SzJ (NSG) mice were purchased from Charles River (France). Mice were bred and maintained in the animal facility of Leiden University Medical Center (LUMC). All animal experiments were approved by the Dutch Central Commission for Animal experimentation (Centrale Commissie Dierproeven, CCD).

Lentiviral vectors and vector production

The *RAG1* gene sequence was optimized as described by Pike-Overzet et al (2011). Briefly, this resulted in 90% of the codons being adapted to the codon bias of Homo sapiens genes. Furthermore, the GC-content was raised from 48 to 61% and the number of cis-acting motifs was reduced from 21 to 0. The optimized *RAG1* sequence was synthesized by GeneArt (Regensburg, Germany). Codon optimized RAG1 (c.o.RAG1) was cloned into self-inactivating lentiviral pCCL plasmid resulting in pCCL-Cbx3.MND.coRAG1 (hereafter: Cbx3.MND-c.o.RAG1), pCCL-MND-c.o.RAG1 (hereafter: MND-c.o.RAG1), pCCL-PGK-c.o.RAG1 (hereafter: PGK-c.o.RAG1) and pCCL-UCOE-c.o.RAG1 (hereafter: UCOE-c.o.RAG1). DNA sequencing of the transgene was performed

to validate the gene transfer constructs. Helper plasmids pMDLg/pRRE, pRSV-Rev and pMD2.VSVG for lentiviral production were kindly provided by L.Naldini (San Raffaele Telethon Institute for Gene Therapy, Milan, Italy) [30]. Large-scale helper-plasmid preparations were obtained through PlasmidFactory (Bielefeld, Germany).

293T cells were transiently transfected with the transfer and helper plasmids using X-tremeGene HP DNA transfection reagent (Sigma-Aldrich). Lentiviruses were harvested 24h, 30h and 48h after transfection, filtered through 0.22µm pore filters (Whatmann) and stored at -80°C. Pooled lentiviral supernatant was concentrated by ultracentrifugation (Beckman Optima^{TM} LE-80K, rotor SW32Ti) for 16 hours at 10.000 rpm and 4°C under vacuum conditions. Pellets were resuspended in StemSpan Serum-Free expansion medium (SFEM; Stemcell Technologies Inc) and aliquoted to avoid multiple freeze/thaw cycles. Since no suitable anti-RAG1 antibodies were available, we determined the viral titer using qPCR as described later on. A clinical GMP-grade vector was generated by Batavia Biosciences (Leiden, The Netherlands), aliquoted in 200 µL vials and stored at -80 degrees until use. The GMP-grade vector was tested and validated on murine Rag1 deficient bone marrow cells, human CD34+ cells.

Transduction of murine lineage negative bone marrow cells and human CD34+ cells

Murine bone marrow (BM) cells were obtained from femurs and tibias of C57BL/6 wild-type and C57BL/6 Rag1$^{-/-}$ mice. The obtained bones were flushed or crushed, cells were passed through a 0,7 µm cell strainer (Falcon), washed and viable frozen. After thawing, lineage negative cells were isolated using mouse lineage depletion kit and AUTOMacs cell sorter (Miltenyi Biotech). Lineage negative cells were stimulated overnight in StemSpan-SFEM containing Penicilin/Steptamycin (5,000 units/5,000 µg/ml; Gibco) and supplemented with 50 ng/mL recombinant mouse FMS-related tyrosine kinase 3 ligand (rmFLT3L; R&D systems), 100 ng/mL recombinant mouse Stem-Cell Factor (rmSCF; R&D systems) and 10 ng/mL recombinant mouse thrombopoietin (rmTPO; R&D systems). Rag1$^{-/-}$ cells were subsequently transduced with the different lentiviruses using 4 ug/ml proteamine sulphate (Sigma-Aldrich) and by way of spin-occulation at 800xg and 32°C for 1 hour. Cells were cultured at 37°C, 5% CO_2 for 24h in medium supplemented with cytokines.

Human bone marrow from children diagnosed with SCID was obtained according to the Medical Ethical Committee and IRB guidelines at Leiden University Medical Center. The patient in this study was a compound heterozygote with the following confirmed mutations: RAG1 allele 1 C 256-257 deletion AA, allele 2 C 1677 G>T. Mononuclear cells were separated by Ficoll gradient centrifugation, frozen in fetal calf serum (Greiner Bio-one)/10% DMSO (Sigma-Aldrich) and stored in liquid nitrogen. After thawing, human CD34^{+} cells were isolated using CD34 MicroBead UltraPure Kit (Milteny Biotec). Enriched CD34+ cells were stimulated overnight in X-VIVO15 without Gentamycin and phenol red (Lonza) -1% human albumin (200 g/L; Sanquin) - Pen/Strep medium supplemented with 300 ng/ml huSCF (Milteny Biotec), 100 ng/ml huTPO (Milteny Biotec), 300 ng/ml huFlt3L (Milteny Biotec) and 10 ng/ml huIL3 (Milteny Biotec). Cells were transduced in X-VIVO-15 complete medium with 4 µg/mL proteamine sulphate as described previously and cultured for 24h.

Transplantation of Rag1$^{-/-}$ and NSG mice

Control mock-transduced cells (C57BL/6 wild-type cells referred as WT control and Rag1$^{-/-}$ cells referred as KO control) and transduced Rag1$^{-/-}$ murine cells (equal amount of cells per group, up to 5*10^5 cells/mouse depending on the experiment) were mixed with supportive Rag1$^{-/-}$ spleen cells (3*10^6 cells/mouse) in Iscove's Modified Dulbecco's Medium (IMDM) without phenol red (Gibco) and transplanted by tail vein injection into pre-conditioned Rag1$^{-/-}$ recipient mice. Recipient mice (8-12 week old mice) were conditioned with a total body single dose irradiation 24h prior the transplantation using orthovoltage X-rays (8.08Gy) or with two consecutive doses of 25 mg/kg Busulfan (Sigma-Aldrich) (48h and 24h prior transplantation).

After overnight culture, 60.000 to 70.000 human CD34$^+$ cells were resuspended in (IMDM) without phenol red (Gibco) and transplanted intravenously into busulfan pre-conditioned NSG recipient mice (5week old mice, busulfan conditioning as described above).

Mice used for transplantation were kept in a specified pathogen-free section. The first four weeks after transplantation mice were fed with additional DietGel recovery food (Clear H2O) and antibiotic water containing 0.07 mg/mL Polymixin B (Bupha Uitgeest), 0.0875 mg/mL Ciprofloxacin (Bayer b.v.) and 0.1 mg/mL Amfotericine B (Bristol-Myers Squibb) and their welfare was monitored daily. Peripheral blood (PB) from the mice was drawn by tail vein incision every 4 weeks until the end of the experiment. PB, thymus, spleen and BM were obtained from CO_2 euthanized mice.

Immunization

Mice were immunized with synthetic TNP-KLH antigen 4 weeks before the end of the experiment. 100 µg TNP-KLH (Biosearch Technologies Inc.) in 50% Imject Alum (Thermo Scientific) was injected intraperitoneal (i.p.). 3 weeks later, mice were boosted i.p. with 100 µg TNP-KLH in PBS. Serum was collected before immunization and 1 week after the boost injection.

Flow cytometry

Single cell suspensions from thymus and spleen were prepared by squeezing the organs through a 70 µM cell strainer (BD Falcon) and single cell suspension from BM was made as described above. Erythrocytes from PB and spleen were lysed using NH_4Cl (8,4 g/L)/$KHCO_3$ (1 g/L) solution. Single cell suspensions were counted and stained with the antibodies listed in **Table S2**. Briefly, cells were incubated for 30 min at 4°C in the dark with the antibody-mix solution including directly conjugated antibodies at the optimal working solution in FACS buffer (PBS pH 7.4, 0.1% azide, 0.2% BSA). After washing with FACS buffer, a second 30 min incubation step at 4°C was performed with the streptavidin-conjugated antibody solution. When necessary, 7AAD (BD Biosciences) was used as viability dye. Cells were measured on FACS-CantoII and LSR Fortessa X-20 (BD Biosciences) and the data was analysed using FlowJO software (Tree Star).

Determination vector copy number (VCN) and c.o.RAG1 expression by RT-qPCR

qPCR was used for the quantitative analysis of genomic lentiviral RNA, proviral DNA copies and transgene mRNA expression using WPRE, c.o.RAG1, ABL and PTBP2 as targets (Table S3). Total RNA from single cell suspensions was purified using RNeasy

Mini kit (Qiagen) and reverse transcribed into cDNA using Superscript III kit (Invitrogen). Genomic DNA was extracted from single cell suspensions using the GeneElute Mammalian Genomic DNA kit (Sigma-Aldrich). Dneasy Blood and Tissue Kit (Qiagen) was used to isolate genomic DNA from murine organs and tissues. VCN was determined on DNA samples by the detection of WPRE and PTBP2. The levels of transgene expression were determined on cDNA samples, by normalizing *c.o.RAG1* to the expression of the *ABL* gene. qPCR was performed using TaqMan Universal Master Mix II (Thermofisher) in combination with specific probes for indicated genes from Universal Probe Library (Roche). Primers and probes used are listed in Table S3. PCR reactions were performed on the StepOnePlus Real-Time PCR system (Thermofisher). All samples were run in triplicate.

Serum immunoglobulin quantification

Murine IgG, IgM, IgE, TNP-specific IgG and human IgM were determined by a sandwich enzyme-linked immunosorbent assay (ELISA). NUNC Maxisop plates (Thermo Scientific) were coated with unlabeled anti-mouse IgG, IgM (11E10), IgE antibodies (SouthernBiotech) or unlabeled anti-human IgM antibody (Jackson Immuno Research laboratories, kindly provided by Dr. Karahan, LUMC). For detection of TNP-specific IgG, plates were coated with synthetic TNP-KLH (Biosearch Technologies Inc.). Blocking was done with 1% BSA/PBS (mouse) or 2% BSA/0.025 Tween/PBS (human) for 1h at room temperature (RT) and subsequently serial dilutions of the obtained sera were incubated for 3h at RT. After washing, plates were incubated with biotin-conjugated anti-mouse IgG, IgM, IgE (SouthernBiotec) or anti-human IgM (Novex life technologies, kindly provided by Dr. Karahan, LUMC) for 30 min at RT. For detection, plates were incubated for 30 min at RT with streptavidin horseradish peroxidase (Jackson Immuno Research laboratories) and subsequently azino-bis-ethylbenzthiazoline sulfonic acid (ABTS, Sigma-Aldrich) was used as a substrate. Data was acquired at a wavelength of 415 nm using Bio-Rad iMark microplate reader and MPM 6 software (Bio-Rad). Antibody concentration was calculated by using serial dilutions of purified IgG, IgM, IgE proteins (SouthernBiotech) and human reference serum (Bethyl Laboratories, kindly provided by Dr. Karahan, LUMC) as standards.

Repertoire analysis

Total RNA was purified from murine spleen cells and reverse transcribed into cDNA as described previously. GeneScan analysis procedure of the murine T-cell repertoire was adapted from [31]. cDNA was amplified using a FAM-labeled C gene segment-specific primer along with 24 TCR Vβ-specific primers (See **Table S3**). GeneScan™ 500 ROX™ (ThermoFisher) was used as internal size standard. Labeled PCR products were run on the ABI Prism® Genetic Analyzer (Applied Biosystems) for fragment analysis. Raw spectratype data was analyzed, visualized and scored by ImSpectR, a novel spectratype analysis algorithm for estimating immunodiversity [32] ImSpectR identifies and scores individual spectratype peak patterns for overall (Gaussian) peak distribution; shape of individual peaks, while correcting for out-of-frame TCR transcripts. Scores range from 0 when no peaks detected, to 100 for a diverse TCR repertoire.

Human immunoglobulin and T-cell receptor repertoire generated in NSG mice was analyzed on DNA samples from BM and thymus (DNA was extracted as described previously). Rearrangements were analyzed using the EuroClonality/BIOMED-2 multiplex PCR protocol [33]. Amplification of IgH, IgK, TCRβ and TCRγ rearrangements were performed following the *IGH* + *IGK* B-Cell Clonality Assay (InvivoScribe) and *TCRB* + *TCRG* T-Cell Clonality Assay (InvivoScribe) instructions respectively. PCR products were analyzed by differential fluorescence detection using ABI-3730 instrument (Applied Biosystems) for fragment analysis. The output files were visualized and analyzed using ImSpectR.

Non-restrictive Linear Amplification Mediated PCR (nrLAM-PCR)

Lentiviral insertion site was analysed by nrLAM-PCR on murine bone marrow DNA samples as described by Schmidt M. et al [34].

In Vitro Immortalization assay (IVIM)

Genotoxic potential of the viral vectors (Cbx3.MND-c.o.RAG1, MND-c.o.RAG1, PGK-c.o.RAG1, UCOE-c.o.RAG1) was quantified as previously described by Baum et al. [35].

Gross pathology and histopathology

A full necropsy was performed, organs were collected subjected to macroscopic and microscopic examination (Table S1 of collected organs). The selection of organs to be examined for gross pathology and histopathology analyses followed the applicable European and international guidelines (EMEA 1995, WHO 2005) [36]. For gross pathology, the external surface of the body, orifices, the thoracic abdominal and cavities were examined (Analyzed organs are listed in Table S1).

For histopathological examination organs were fixed in 4% neutral buffered formalin for 24 hours and paraffin embedded, 5 µm sections were processed for hematoxylin and eosin (HE) and for immunohistochemistry stainings according to standard procedures [37]. All slides were examined blindly by a European board certified pathologist (ECVP).

Before staining, paraffin sections were deparaffinated. Antigen retrieval was performed for antibody against FOXP3 and Cytokeratin 5/6 by heating during 12 minutes at 98 ^{0}C in citric acid buffer (0,01 Mol/L, pH 6,0). Inhibition of endogenous peroxidase was done in 0.3% H_2O_2 in PBS. After incubation overnight at room temperature with antibody against FOXP3 (1/70, 700914; Thermo Scientific, Waltham, MA, USA) and Cytokeratin 5/6 (1/100, GA780; DAKO, Glostrup, Denmark) the secondary antibody biotinylated Goat anti Rabbit IgG (1/200, BA-1000; Vector Labs, Burlingame, CA USA) and biotinylated Horse anti Mouse (1/200, BA-2000; Vector Labs, Burlingame, CA USA) was incubated for 90 minutes. Visualization was enforced with ABC staining kit (Vectastain ABCkit, HRP, PK6100, Vector Labs, Burlingame, CA USA) for 45 minutes. As substrate for horseradish peroxidase 3,3'-diaminobenzidine tetrahydrochloride (DAB, D5637, Sigma-Aldrich, St Louis, MO USA) was applied for 10 minutes. Mayer's hematoxylin was utilized as nuclear counterstaining.

Statistics

Statistics were calculated and graphs were generated using GraphPad Prism6 (GraphPad Software). Statistical significance was determined by standard one/two-tailed Mann-

Whitney U test, ANOVA test or two-tailed non-parametric Spearmen correlation (*p<0.05, **p < 0.01, ***p < 0.001 and ****p<0.0001).

RESULTS

MND promoter as most optimal vector to correct Rag1 deficiency.

At the onset of this project we constructed four different SIN LV transfer plasmids in the CCL backbone and tested four different promoters: PGK (Human PhosphoGlycerate Kinase (PGK)-1 promoter, nucleotides 5 to 516; GenBank accession no.M11958; [30], MND (myeloproliferative sarcoma virus enhancer, negative control region deleted, dl587rev primer binding site substituted promoter; [38], UCOE (the modified chromatin-remodeling element, devoid of unwanted splicing activity and minimized read-through activity; [39],and a tandem combination of UCOE and MND (Cbx3.MND) were used to drive expression of a codon optimized version of the RAG1 (**Fig 1A**).

Recombinant lentiviruses were produced at small and large scale to evaluate virus production and in vitro expression efficiency of the different vectors. The transfer vectors in conjunction with GAG-Pol, REV and VSV-G plasmids were transiently transfected into 293T cells to produce the different lentiviruses. The number of infectious particles of the small and large virus batches was assessed before and after concentration by Q-PCR. Consistently, both the small and large batches of UCOE-c.o.RAG1 lentivirus (both unconcentrated and concentrated) had a significantly lower number of infectious genomes per mL compared to the other vectors (**Fig 1B** and **Fig 1C**), highlighting a difficulty to scale up its production. These lentiviruses were subsequently used to transduce lineage negative bone marrow (BM) cells from Rag1-deficient mice in order to determine their functional characteristics under conditions relevant for in vivo application. We found that UCOE-c.o.RAG1 reached lower VCN (**Fig 1D**) than the other vectors and PGK-c.o.RAG1 was the vector with lowest promoter strength (**Fig 1F**). Unfortunately, both PGK and UCOE-c.o.RAG1 only resulted in low levels of c.o.RAG1 expression (**Fig 1E**) whereas quite high levels are known to be required for immune reconstitution [24, 40, 41]. Indeed, an in vivo pilot experiment where Rag1-deficient mice were transplanted with wild-type (WT) stem cells, mock transduced Rag1-deficient stem cells or gene therapy treated stem cells using the four different promoters, revealed that the promoter strength and essentially the level of c.o.RAG1 is crucial to obtain adequate immune reconstitution (2 independent pilot experiments, total 6 or 7 mice per group). Immune reconstitution of these mice was followed in the peripheral blood every 4 weeks, showing that B-cell and T-cell reconstitution were achieved in the different gene therapy group to different extents (**Fig S1A**). Reflecting the known promoter strengths of these four vectors, a wide range of c.o.RAG1 expression was created by this initial experiment. Interestingly, 16 weeks after transplantation, we observed a clear linear correlation between the expression of c.o.RAG1 achieved in the BM and the number of B cells (B220+IgM+ cells) generated (**Fig 1G,** left and middle panel). For T cells, we observed that there was a threshold of minimal c.o.RAG1 expression to develop an active double positive CD4 and CD8 (DP) population in the thymus, roughly at 10x the house keeping control level (**Fig 1H**, left and middle panel). Mice reconstituted with stem cells having lower c.o.RAG1 expression than this

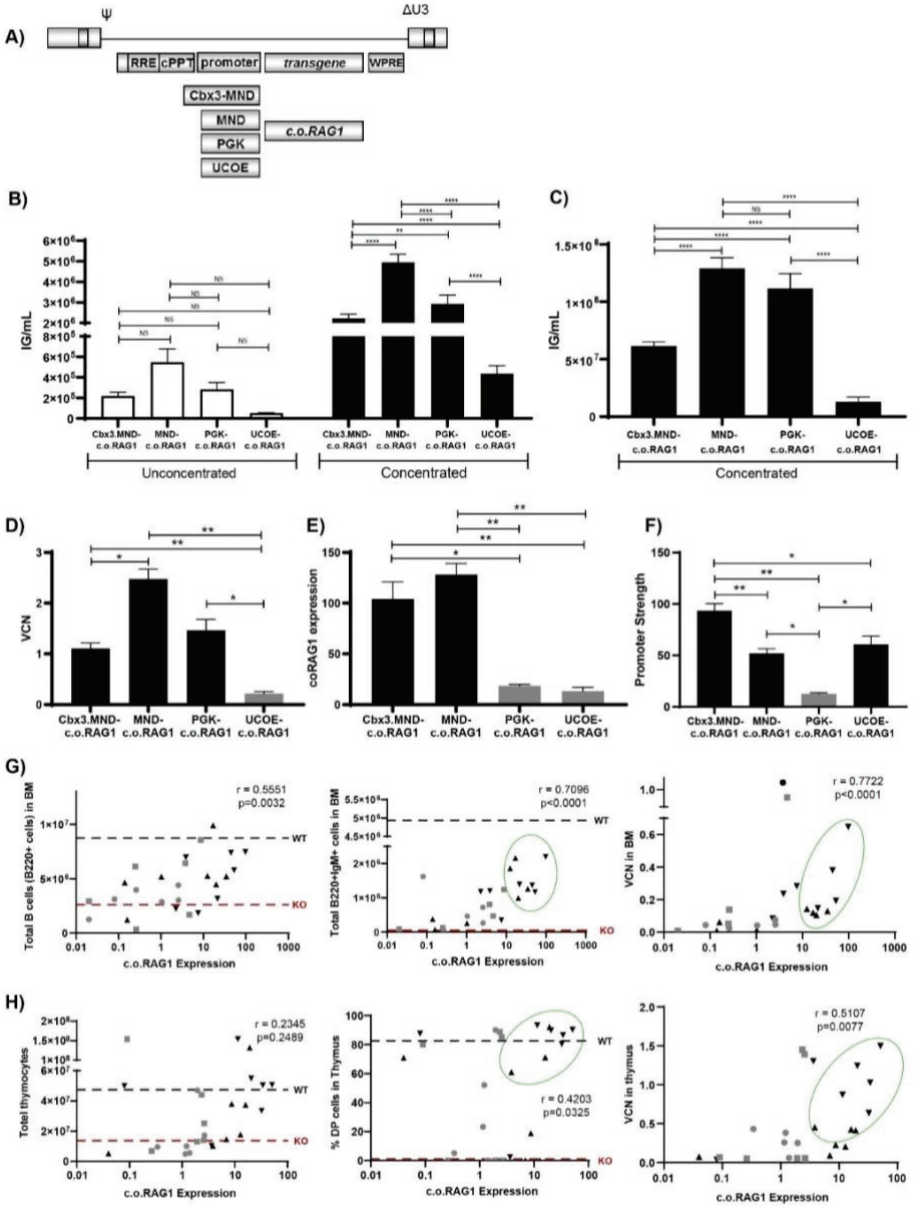

Figure 1: Selecting the Optimal SIN LV Plasmid: Virus Production and In Vitro Efficiency. *(A) Four different SIN LV plasmids in the CCL backbone carrying different promoters (Cbx3.MND, MND, PGK, and UCOE promoter) were tested to drive expression of a codon-optimized version of RAG1. (B) Production of lentivirus batches with the different constructs. The number of infective particles (infectious genomes/mL) from unconcentrated and concentrated small batches was determined. Three independent lentivirus small batches per plasmid were produced and analyzed (two-way ANOVA test; *p < 0.05, **p < 0.01). (C) Production of lentivirus batches on a large scale with the different constructs. The number of infectious genomes/mL after concentration of large lentiviruses*

*batches was determined. (D) Transduction efficiency of the different SIN lentiviruses in murine lineage-negative cells. VCN was determined by WPRE determination on genomic DNA. Three independent lentivirus batches per plasmid were produced and analyzed (one-way ANOVA test; *p < 0.05, **p < 0.01. (E) Determination of transgene expression in the transduced cells by the different constructs. c.o.RAG1 expression relative to ABL1 was determined by qPCR. Three independent lentivirus batches per plasmid were produced and analyzed (one-way ANOVA test; *p < 0.05, **p < 0.01. (F) Determination of the promoter strength (c.o.RAG1 expression/VCN) of the different plasmids. Three independent lentivirus batches per plasmid were produced and analyzed (one-way ANOVA test; *p < 0.05, **p < 0.01). (G) Total number of B220+ cells (left panel) and total number of B220+IgM+ cells (middle panel) correlated with the expression of c.o.RAG1 in BM. The correlation between VCN and c.o.RAG1 expression in BM of immune reconstituted mice is shown (right panel) (:, Cbx3.MND; ;, MND;-, PGK;C, UCOE promoters; gray indicates low-expressing plasmids; black indicates high0expressing plasmids; green circles indicate mice with acceptable immune B and T cell reconstitution). Data shown represent two independent in vivo experiments with in total six or seven mice per group. Each dot represents one mouse. Nonparametric Spearman r correlation, two-tailed; **p < 0.01, ***p < 0.001, ****p < 0.0001. (H) Correlation between total thymocytes (left panel) and DP cells (middle panel) with c.o.RAG1 expression in the thymus. Correlation between VCN and c.o.RAG1 expression in the thymus of immune reconstituted mice (right panel) (:, Cbx3.MND;;, MND;-, PGK;C, UCOE promoters; gray indicates low-expressing plasmids; black indicates high-expressing plasmids; green circles indicate mice with acceptable immune B and T cell reconstitution). Data shown represent two independent in vivo experiments with in total six or seven mice per group. Each dot represents one mouse. Nonparametric Spearman r correlation, two-tailed; **p < 0.01, ***p < 0.001, ****p < 0.0001.*

threshold barely reconstituted thymic T-cell development. Accordingly, B- and T-cell reconstitution was consistently achieved in the BM and in the thymus when c.o.RAG1 expression at 10x the house keeping control level or higher which could be achieved. This expression level was mainly reached with VCN's of 1 and lower (**Fig 1G&H,** right panels) using the high expressing vectors such as Cbx3.MND and MND-c.o.RAG1 (black symbols in **Fig. 1G&H**). We considered mice achieved immune reconstitution when B- and T-cell development was successful (overcoming the early developmental block), the cells were functional, with a diverse TCR Vβ repertoire and without signs of toxicity or adverse side effects (**Fig 1G&H,** green circle). In the low *c.o.RAG1* expression mice (grey dots, mainly PGK and UCOE promoter), we found a number of mice (n=4 out of 9) that developed skin rashes and wasting during the course of the experiments which resulted in the death of some mice (similar to the features due to low RAG1 activity described previously [27]), while the animals in the higher *c.o.RAG1* expression group (black dots,Cbx3.MND and MND promoter) as well as the animals that received wild-type cells or uncorrected Rag1 knock-out cells did not display any health problems. Collectively, our *in vitro* and *in vivo* pilot data highlight the importance of achieving sufficient *c.o.RAG1* expression, at VCN around or below 1, in order to obtain successful immune reconstitution, which was only accomplished using Cbx3.MND-c.o.RAG1 and MND-c.o.RAG1 lentiviruses (**Fig S1B**).

To better compare both vectors, an additional *in vivo* reconstitution experiment was done, with more comparable VCNs. Rag1-deficient mice transplanted with WT stem cells, mock transduced Rag1 KO stem cells, Cbx3.MND-c.o.RAG1 (starting VCN = 0.95) or MND-c.o.RAG1 (starting VCN = 1.1) treated stem cells were extensively analyzed 16 weeks

after transplantation by flow cytometry and qPCR for viral copy number (VCN) measuring WPRE (Woodchuck Hepatitis Virus Posttranscriptional Regulatory Element and expression of the therapeutic gene c.o.*RAG1.* Mice were sacrificed after 4 months and immune organs were analysed by flow cytometry (pilot experiment with a total of 3 mice per group). Restoration of IgM+B220+B cells (**Fig 2A**) in the BM was seen in mice treated with WT stem cells and MND-c.o.RAG1 treated gene therapy mice and occasionally in mice with Cbx3.MND elements, even with comparable VCN. Mock transduced Rag1 KO stem cells did not restore B-cell development, where cells were blocked at the pre B cell stage, as expected. In contrast, in gene therapy treated mice the arrest in B-cell development was alleviated, and immature and mature B cells developed (**Fig 2B,** left panel). MND-c.o.RAG1 gene therapy mice successfully developed all B-cell developmental subsets in the BM, similarly to WT transplanted mice and significantly different from the mock KO transplanted mice. We observed that even though B-cell development in BM was satisfactory, B cells numbers detected in the peripheral blood were significantly lower than in the WT situation (**Fig 2B,** right panel). However, B cell functionality was fully restored to WT degree as the levels of immunoglobulins (IgG and IgM) detected in serum were comparable to WT transplanted mice (**Fig 2G**). We next analysed the thymus for T-cell marker-expression, using (amongst other markers) CD4 and CD8. Proper T-cell development with a full spectrum of DP and single positive CD4 or CD8 (SP) developmental stages was observed with WT and MND-c.o.RAG1 cells, but not with Cbx3.MND-c.o.RAG1 cells where mice showed an exhausted thymus phenotype with mature CD4 and CD8 SP cells but not DP cells anymore 16 weeks after transplantation (**Fig 2C&D**). Similar to B cells, the total number of T cells in the periphery was lower than in mice treated with WT cells; nonetheless mature T cells after gene therapy showed a diverse T cell receptor (TCR) repertoire. We used GeneScan analysis for 24 different Vβgenes and calculated the cumulative complexity score. As shown in the representative plots (**Fig 2E**) as well by the ImSpectR score (**Fig 2F**), the MND promoter performed closer to WT treated mice, revealing an active V(D)J recombination machinery able to successfully rearrange *TCR* genes.

Besides efficacy, safety is an important aspect for clinical use of gene therapy vectors. As an additional selection criterion our research grade lentivirus batches were tested in the IVIM assay, which is the currently accepted (FDA and EMA approved) standard assay for safety of viral vectors. Even though high VCN per cells were achieved in this assay with the test vectors, both vectors were shown to have a frequency of insertional mutagenic events, that were at least 50 fold lower than classical RSF91 gamma-retroviral vectors with known mutagenic potential (**Fig 2H**). In three independent IVIM assays, we did not observe cytotoxicity of the vector supernatants on lineage negative bone marrow cells.

This safety selection criterium, together with the successful *in vivo* immune reconstitution given by the MND-c.oRAG1 treated cells (**Fig S1C**), led us to conclude that the pCCL-MND-c.o.RAG1 LV vector is the best vector of choice and we therefore proceeded to have the vector produced at GMP grade. All following experiments described were conducted with this clinical grade vector for further preclinical testing.

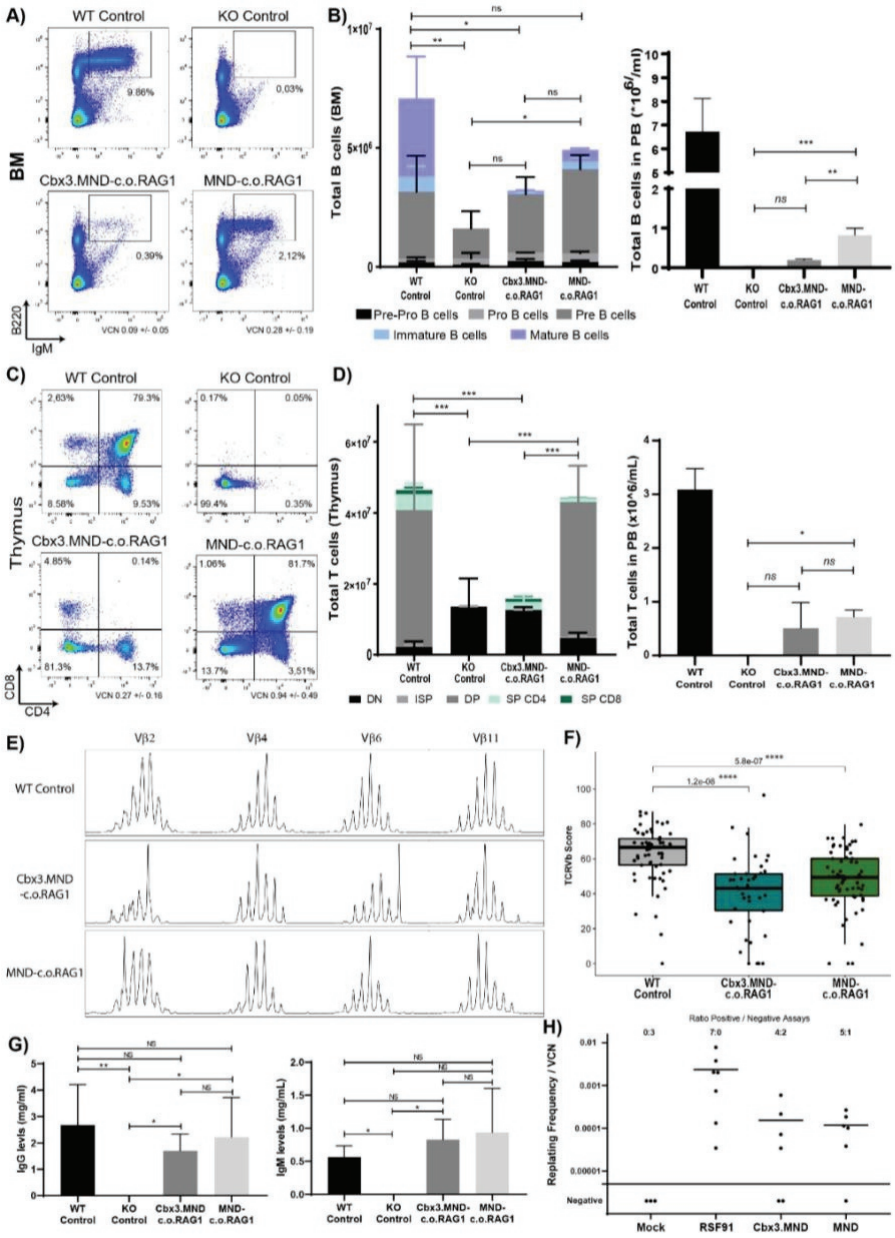

Figure 2: Selecting the Optimal SIN LV Plasmid to Drive an Immune Reconstitution of Rag1 Deficiency. *Rag1-deficient mice (experiment with a total of 3 mice/group) were transplanted with 500,000 stem cells: WT cells, mock Rag1 KO cells, Cbx3.MND-c.o.RAG1-treated KO cells (VCN of 0.95), and MND-c.o.RAG1-treated KO cells (VCN of 1.1). (A) Representative FACS plots showing the restoration of B220high+ B cells in the BM. (B) Total number of the different B cell subsets in the BM (left panel) and total number of B cells (B220high+) in the PB (right panel) 16 weeks after SC*

*transplantation. Graphs represent the means and standard deviation of a pilot experiment with two to three mice per group (Mann-Whitney test, one-tailed; *p%0.05; NS, not significant). (C) Representative FACS plots of the thymus reconstitution (CD4 versus CD8) with the different constructs. (D) Total number of the different T cell subsets in the thymus (left panel) and total number of T cells (CD3+TCRab+) in PB (right panel) 16 weeks after transplantation. Graphs represent the means and standard deviation of a pilot experiment with two to three mice per group (Mann-Whitney test, one-tailed; *p % 0.05; NS, not significant). DN, double negative; ISP, immature single positive; DP, double positive; SP, single positive. (E) Representative samples of GeneScan plots are shown for four different families (x axis indicates CDR3 length; y axis shows the fluorescence intensity of the runoff products). (F) TCR Vb repertoire analysis by GeneScan. A total of 24 Vb families were analyzed on spleen cells from three mice per group. Overall score of all of the families was calculated for the different constructs (Mann-Whitney test; p values are represented on the plot; ****p < 0.0001; NS, not significant). (G) Quantification of total IgG and IgM in mice serum by ELISA (one-way ANOVA test; *p < 0.05, **p < 0.01). (H) IVIM assay was performed on the two constructs to assess their safety (mock cells as negative control; RSF91 g-retroviral vector as a positive control). Data show results from three complete IVIM assays.*

Extensive preclinical testing of the pCCL-MND-c.o.RAG1 LV vector in Rag1-/- mice.

Initial analysis of 8 *Rag1*-/- mice treated with the MND vector (starting VCN = 0,2), positive (WT stem cells; 3 mice) and negative controls (mock transduced Rag1-/- stem cells; 3 mice) 24 weeks after transplantation confirmed good B-cell reconstitution in the periphery (PB) and in BM (**Fig 3A**), although the numbers remained lower than mice treated with WT stem cells (**Fig 3B** and **Fig S2A**), which could be due to partially arrested development from pre-B to immature B-cell stages (**Fig S2B**) originating from cells that were transduced with insufficient levels of c.o.RAG1 to support full Ig rearrangements. Alternatively, residual pro- and pre-B cells could inhibit B-cell development by occupying important developmental niches. However, gene therapy mice showed similar proportion of immature and mature B-cell subsets in the spleen (**Fig 3C**). Concerning T-cell reconstitution, most GT mice showed next to complete thymic T-cell development with thymocyte numbers almost normal (**Fig 3D** and **Fig S2A&B**), although the T-cell numbers in the periphery were restored to ~30% of normal levels (**Fig 3E**), with somewhat lower proportion of naïve CD4 and CD8 T cells and increased effector memory subsets (**Fig 3F**), most likely due to homeostatic proliferation from initial T cell that egressed from the thymus. Indeed, delayed T-cell development can be observed in the GT mice compared to WT controls (**Fig S2A&B**) and therefore the proportions of naïve and memory T cells might still not be entirely balanced after GT. Besides analysing the primary and secondary immunological organs by flow cytometry, we also checked restoration of the immune system by histological analyses. Spleen, lymph nodes and thymus showed remarkably normal architecture after GT (**Fig 3G**), comparable to mice treated with WT stem cells, and quite different from the negative control mice treated with mock transduced Rag1-/- cells. Importantly, restoration of FoxP3 expression which directs T cells into the CD4+ regulatory T cell lineage (Treg) was also observed in mice treated with MND-coRAG1 gene therapy (**Fig 3G**).

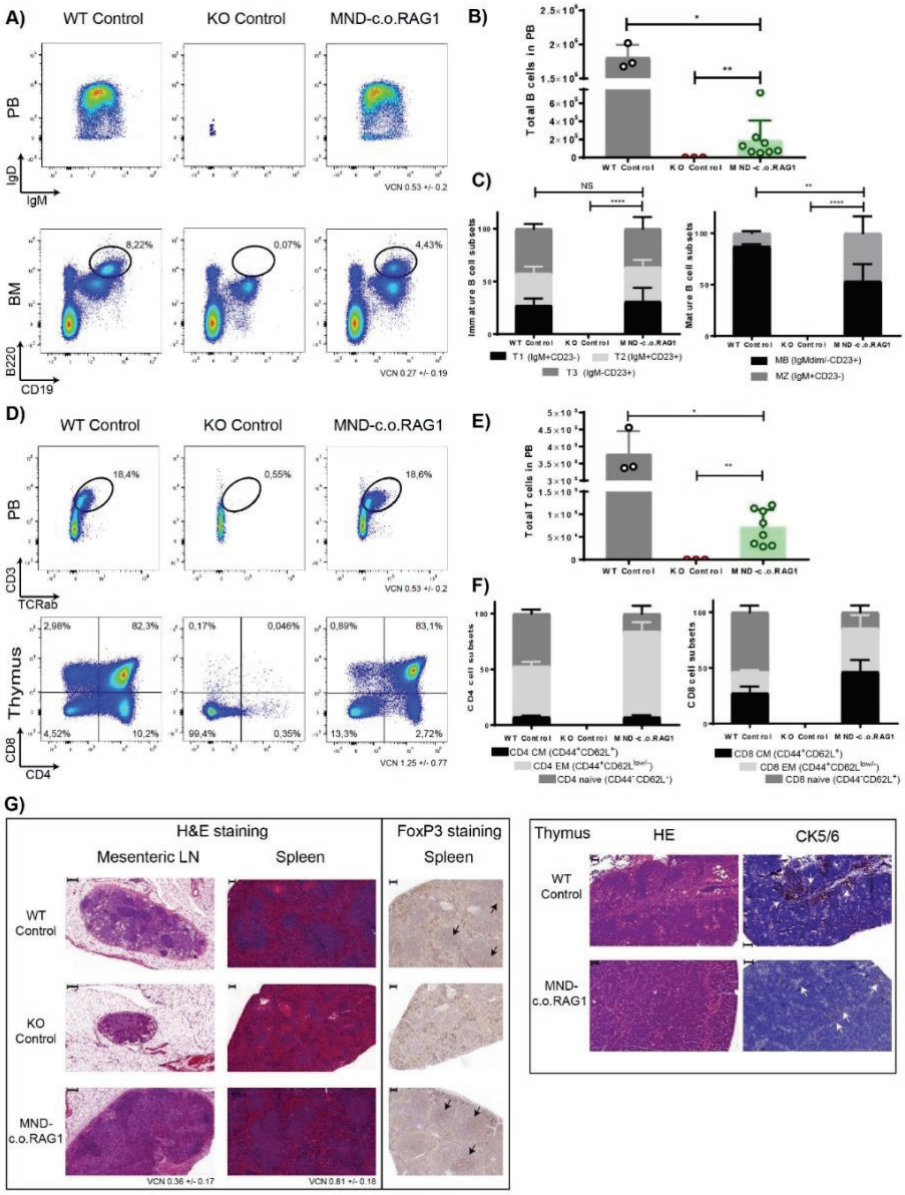

Figure 3: Extensive Immune Reconstitution of Mice Receiving Gene Therapy of Stem Cells with a Clinical-Grade MND-c.o.RAG1 Vector. *Rag1-deficient mice were transplanted with 250,000 stem cells: WT cells (three mice), mock KO cells (three mice), and MND-c.o.RAG1-treated cells (VCN of 0.2; eight mice). (A) Representative plots of B cell reconstitution in the blood (B220+IgM/IgD cells; top panel) and B cell development in the BM (B220+CD19+ cells; bottom panel) 24 weeks after transplantation. (B) Total number of B cells (B220+CD11b/CD43_ cells) in the PB (Mann-Whitney test, one-tailed; *p < 0.05, **p < 0.01). (C) Immature (B220+CD93+ cells; left panel) and mature (B220+CD93- cells; right panel) B cell subsets distribution in spleen. Two-way ANOVA test; ***p <*

*0.001; ****p < 0.0001. (D) Representative plots of T cell reconstitution in the blood (CD3+TCRab+ cells; top panel) and T cell development in the thymus (CD4 versus CD8 cells; bottom panel) 24 weeks after transplantation. (E) Total number of T cells (CD3+TCRab+ cells) in PB at the end of the experiment (24 weeks) (Mann-Whitney test, one-tailed; *p < 0.05, **p < 0.01). (F) Naive, effector memory (EM), and central memory (CM) subset distributions for CD4 (CD3+TCRab+CD4+; left panel) and CD8 (CD3+TCRab+CD8+; right panel). T cell subset distributions in spleen are shown: naive cells (CD44_CD62L+), EM cells (CD44+CD62L-) and CM cells (CD44+CD62L+) 24 weeks after transplantation. (G) Left panel: Hematoxylin and eosin staining of mesenteric lymph nodes (scale bars, 200 mm) and spleen (scale bars, 100 mm; purple indicates germinal centers, and red indicates red pulp). Representative FoxP3 staining in spleen tissue (scale bars, 100 mm) is shown. Arrows indicate positive FoxP3 in germinal centers. Representative images are from WT control, KO control, and MND-c.o.RAG1 gene therapy mice. Right panel: Histological analysis of thymus reconstitution by hematoxylin and eosin staining (scale bars, 50 mm) and cytokeratin 5/6 staining (scale bars, 100 mm) . Representative images from WT control and MND-c.o.RAG1 mice. KO thymus was completely used for phenotyping (FACS, DNA, RNA), but KO thymic histology was previously described by van Til et al.[27]*

Functional reconstitution of immunity after Rag1 gene therapy

Next, we tested if the T and B cells that developed had a diverse repertoire and were capable of mounting an immune response against a T cell dependent neo-antigen. GeneScan analysis (3 WT control mice, 1 KO control mouse and 8 MND-c.o.RAG1 mice) showed a diverse TCR Vβ repertoire, that was slightly less complex before immunization than in mice reconstituted with WT stem cells (**Fig 4A**), but after immunization there was no statistical difference in immune repertoire. Total IgM, IgG and IgE levels were also checked (**Fig 4B** and **Fig S2D**) and reached close to normal levels in GT treated mice. Therefore, although GT mice were lagging behind with regard to B-cell numbers, their functionality in the form of antibody production was restored to WT levels. We used TNP-KLH as T-cell specific antigen and measured the production of TNP specific IgG antibodies, thereby investigating whether the developed T and B cell could collaborate in an active immune response. The TNP-specific IgG levels in serum were similar between mice treated with WT stem cells and GT treated mice (**Fig 4C**), showing the potential of a robust immune response after GT.

Pre-clinical release tests of the vector

As required by regulatory authorities the clinical grade vector was tested by external parties for the presence of replication competent virus (RCL). The vector tested negative in two independent tests (data not shown). Other release tests that are commonly required included biodistribution of the vector *in vivo*, checking of vector insertion sites, especially on possible clonal outgrowth, and tests for insertional mutagenesis such as IVIM.

We checked vector distribution on a large number of perfused organs (**Table S1**) in all GT treated mice (a total of 8 mice; **Fig 5A**). Perfusion was used to remove most of the blood cells, in which the leukocytes should carry the vector. As expected, given the positive selection for c.o.RAG1 transduced cells, high VCN was found in the thymus, followed by other immune organs, spleen, bone marrow, lymph nodes and peripheral blood. All other organs had very low signals, except some incidental positivity in stomach and lungs, possibly due to incomplete perfusion, or an ongoing infection in rare individual mouse.

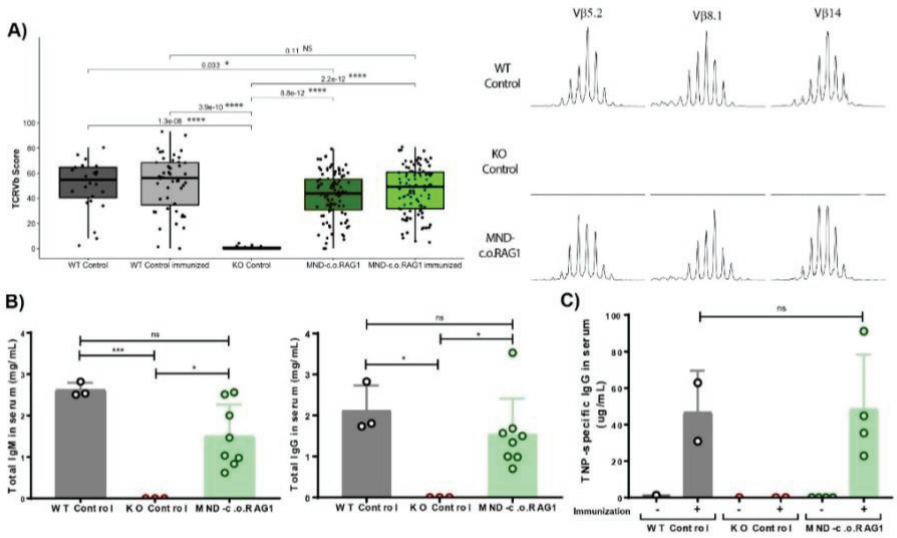

Figure 4: Functional Ig and TCR Rearrangements and Ig Class-Switch after RAG1 Gene Therapy*. (A) TCR Vb repertoire analysis by GeneScan from three WT control mice, one KO control mouse, and eight MND-c.o.RAG1 mice. A total of 24 Vb families were analyzed on spleen cells from three WT control, one KO control, and eight MND-c.o.RAG1 mice (non-immunized and immunized). Overall score of all of the families was calculated by ImSpectR (Mann-Whitney test; p values are represented in the plot; *p < 0.05, ****p < 0.0001; NS, not significant). Representative samples of GeneScan plots are shown for three different families (x axis indicates CDR3 length; y axis shows the fluorescence intensity of the runoff products). (B) Quantification of total IgG and IgM in serum by ELISA (three mice/control group, eight MND-c.o.RAG1 mice) (one-way ANOVA test; *p < 0.05). (C) Quantification of TNP-specific IgG in serum of immunized mice. Each dot represents a value obtained in one mouse (three mice/control group, eight MND-c.o.RAG1 mice) (one-way ANOVA test; *p < 0.05).*

Importantly, pathological examination of histology slides of 29 different organs per mouse (n=14) did not show any abnormalities in mice treated with MND-c.o.RAG1 gene therapy (Examples of 4 organs shown in **Fig S2C**). Indeed, no signs of Omenn syndrome such as skin rashes, high IgE levels, oligloclonal TCR Vβ repertoire or T cell infiltrates in the skin were detected in the immune reconstituted mice.

Next, we checked viral insertion sites using nrLAM-PCR (Fig 5B), a sensitive technique that can detect clonal insertions as discrete bands, which can then be sequenced if needed.[34]. We invariably found a smear of bands indicating polyclonal haematopoiesis with very little indication of oligoclonality, except for a few minor bands from which we could not get extra specific insertion site information by sequencing. We conclude that there was no evidence of vector-induced clonal selection. This is in line with findings by others on using SIN LV vectors in HSCs. Safety of the clinical grade MND-c.o.RAG1 was also tested using the IVIM assay. The clinical vector showed no clonal outgrowth in different independent experiments, close to results from mock-transduced cells (**Fig 5C**). This is better than the research grade vector presumably due to higher purity resulting in a better functional titer leading to fewer side effects after transduction.

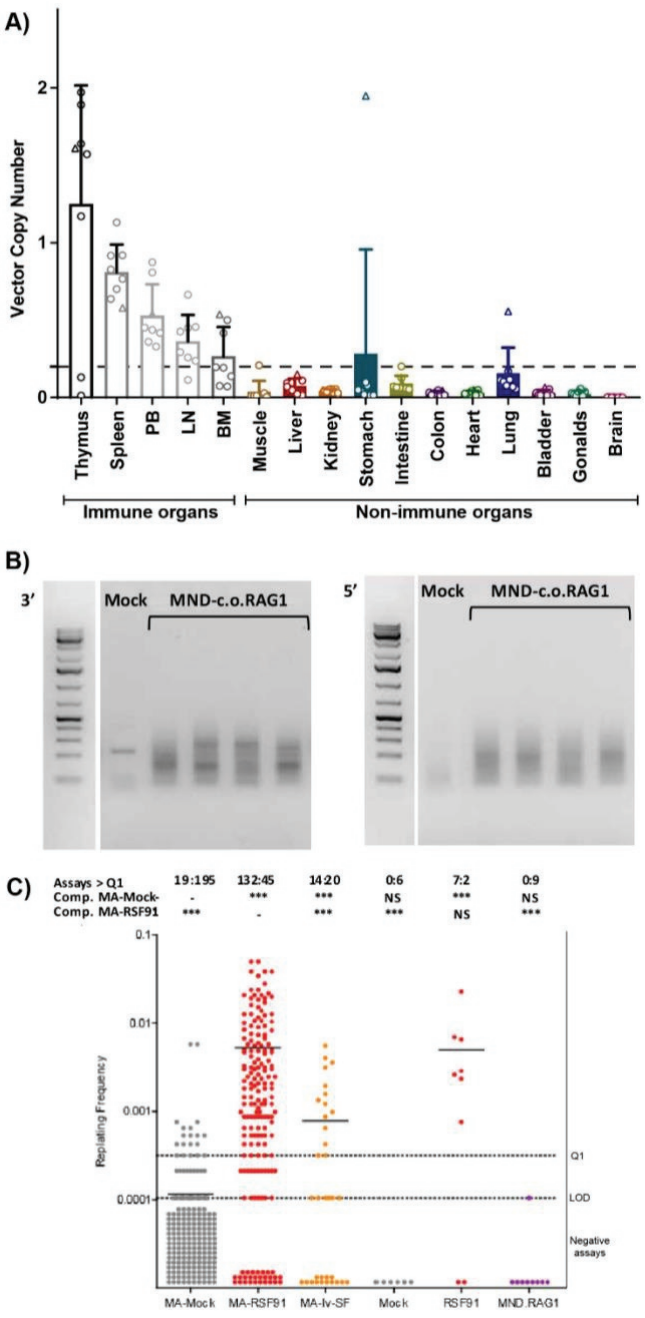

Figure 5: Preclinical Safety Testing of the Clinical-Grade. *(A) Vector biodistribution in immune and non-immune organs assessed by qPCR on DNA samples from 16 organs in total. Each dot represents a value from one mouse (three mice/control group, eight MND-c.o.RAG1 mice). The horizontal dashed line represents the threshold of the VCN of immune organs versus non-immune organs (starting VCN of transplanted cells of 0.2). (B) LV insertion site analysis by nrLAM-PCR of isolated DNA from BM obtained from Rag1-/- untransduced control mouse (mock) and four MND-c.o.RAG1 mice (male non-immunized/immunized, female nonimmunized/immunized). Gels shows results of the linear amplification from the 3₀ long terminal repeat (LTR) and 5₀ LTR, respectively (L = 1 kb plus marker). (C) Replating frequencies (RFs) of the control samples mock or RSF91 and the test vector MND-c.o.RAG1, in comparison to data of a meta-analysis for control samples (Mock-MA, RSF91-MA, lv-SF-MA [a lentiviral vector with an SFFV promoter]). The data points below the limit of detection (LOD; plates with no wells above the MTT threshold) were manually inserted into the graph (due to the logarithmic scale of the y axis). Above the graph, the ratios of positive (left number) and negative plates (right number) according to the MTT assay are shown. Differences in the incidence of positive and negative assays relative to Mock-MA or RSF91-MA were analyzed by Fisher's exact test with a Benjamini-Hochberg correction (*p < 0.05, **p < 0.01, ***p < 0.001; NS, not significant). If above the LOD, bars indicate the mean RF.*

Restored B- and T-cell development in RAG1-SCID patient cells

We have previously shown that transplantation of BM CD34+ cells from SCID patients in NSG mice is informative for identifying where T-cell development is arrested in human SCID [42, 43]. This same model should also be suitable as preclinical efficacy model with patient cells. Hence, we purified CD34+ cells from cryopreserved BM cells from a RAG1-SCID patient. The patient was hypomorphic, with some residual B cells but no T cells. We transplanted busulfan-conditioned mice with either mock transduced or MND-c.o.RAG1 transduced CD34+ cells (1 mouse per group; starting VCN = 0.2) and followed the development of T and B cells over time up to 24 weeks. Human cell engraftment was similar between mice transplanted with gene therapy treated cells and mock transduced cells, indicating that gene therapy did not affect the engraftment of human cells (**Fig S3A**). As expected from the patient phenotype, B cells were observed in the mock transduced humanized mouse, but much higher numbers of B cell were found in the spleen of the GT treated mouse (**Fig 6A** and **Fig S3B**). The B cells that were present also showed polyclonal Ig rearrangement (**Fig S3E**) and produced immunoglobulins, as human IgM could be detected in the sera of the mice (**Fig 6D**), with a tendency towards a more polyclonal repertoire after GT.

Importantly, while no T cells developed in the mouse transplanted with mock transduced RAG1-SCID cells, the gene therapy mouse showed clearly detectable T-cells in PB (**Fig.6B** and **Fig S3C**). After scarifying the mice, we also checked their thymi. As the patient was hypomorphic, we observed that some stages of T-cell development were present, including all double negative (DN; $CD4^-CD8^-$ cells), immature single positive (ISP; $CD4^+CD8^-CD3^-$ cells) and the early CD3- DP stages (**Fig. 6C** and **Fig S3D**). However, there were no cells that were CD3+, so no late CD3+ DP thymocytes, or any SP thymocytes, suggesting that especially the rearrangement of TCRα was affected by this RAG1 mutation. Although immune reconstitution was still not optimal, likely due to the low VCN achieved in that experiment, lentiviral RAG1 GT of CD34+ Rag1-SCID patient cells allows alleviation of the T-cell developmental block and to generate an active thymus. Moreover, human cell engraftment and peripheral B and T cell levels after GT was close to healthy BM CD34+ cell transplantation described in previous work [42]. Finally, we checked *TCRB* and *TCRG* rearrangements by GeneScan analysis. Because of the very limited amount of DNA material, not all possible Vγ and Vβ genes could be analysed, but the selected gene segments showed many more in frame rearrangements in the gene therapy treated group for *TCRG*, while for *TCRB* only in the GT group, rearrangements could be detected (**Fig 6E**). nRLAM_PCR on BM cells revealed a polyclonal pattern with no signs of clonal dominance (**Fig. 6F**).

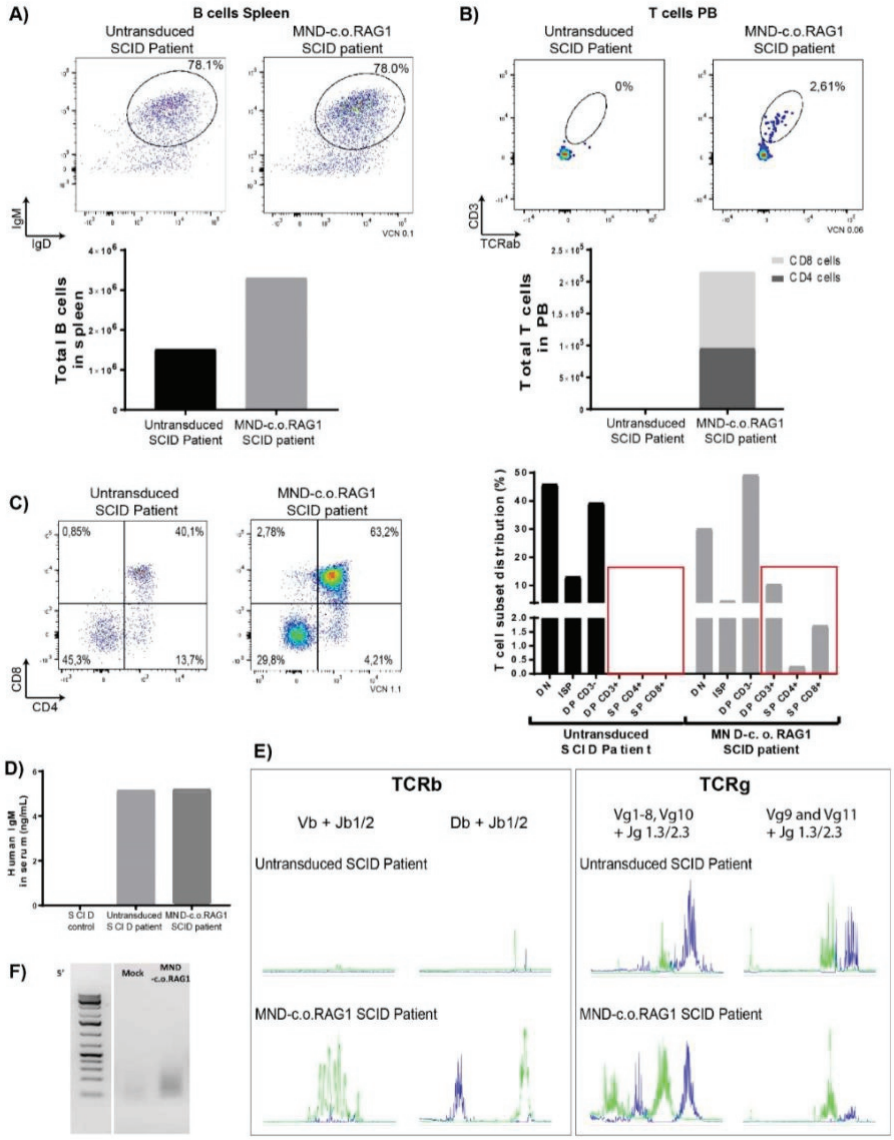

Figure 6: Restored T Cell Development in RAG1 SCID Patient Cells. *65,000 human CD34+ cells were transplanted intravenously into busulfan pre-conditioned NSG recipient mice (one NSG mouse with untreated cells and one NSG mouse with MND-c.o.RAG1 gene therapy cells with a VCN of 0.1). (A) FACS plots of human B cells (CD13/33 CD19+CD20+ cells; top panel) and total number of B cells (CD13/33 CD19+CD20+IgD/IgM cells; bottom panel) in the spleen at week 24 after transplantation. (B) FACS plots of human T cells (CD3+TCRab+; top panel) and total number of T cells, CD4 cells, and CD8 T cells in the PB at week 24 after transplantation (bottom panel). (C) Human T cell development in the thymus: FACS plots (CD4 versus CD8) and distribution of the different T cells subsets in the thymus (24 weeks after transplantation) are shown. (D) Quantification of total human IgM by ELISA of serum from a control NSG mouse transplanted with RAG1-SCID control untreated CD34+ cells*

(non-hypomorphic), our SCID patient CD34+ cells, and our SCID MND-c.o.RAG1 CD34+ cells. (E) Human TCR Vb and Vg repertoire analysis of isolated DNA from NSG thymus (SCID patient and SCID MND-c.o.RAG1) using a TCRB + TCRG T cell clonality assay (x axis indicates fragment sizes; y axis shows the fluorescence intensity of the runoff products). (F) LV insertion site analysis by nrLAM-PCR of isolated DNA from BM obtained from NSG SCID patient untransduced cells (mock) and NSG SCID MND-c.o.RAG1 mice. Gel shows results of the linear amplification from the 5₀ LTR (L = 1 kb plus marker). Data are from an independent experiment with n = 1 per condition.

DISCUSSION

Patients with RAG1-SCID are hampered in the genetic assembly of TCRs and BCRs. Affected children typically experience a wide range of serious, life-threatening infections. Replacing the affected bone marrow with healthy, unmodified, allogeneic stem cells is currently the only therapy for RAG1-SCID. Although overall survival is satisfactory in matched-donor SCT, the outcome in mismatched donor SCT, which represent the majority of cases, is significantly worse. Moreover, approximately 25% of allogeneic SCT-treated patients develop graft vs. host disease, which significantly impairs outcome in terms of morbidity, immune reconstitution, and transplant-related mortality [44]. Additionally, transplant outcome in RAG-SCID (and other recombination-defective forms of T-B-SCID) is significantly worse than for SCID with B cells (i.e. T-B+ SCID) [44, 45]

Transplantation of genetically corrected autologous HSCs, eliminates the risks associated with allogeneic stem cell transplantation (GvHD and rejection) and would therefore provide a valuable alternative particularly for patients lacking a matched donor. Gene therapy for X-SCID with LV or RV SIN vectors has shown to be successful and to lack the xenotoxicity problems previously observed when using γ-retroviral vectors [46, 47, 48]. For ADA-SCID, both RV vectors (currently marketed as approved therapy under the name Strimvelis) and LV vectors have shown excellent clinical results which are comparable to HSCT with matched donors [10, 49, 50.]

Unlike X-linked SCID and ADA-SCID, developing gene therapy for RAG-SCID has been notoriously difficult. Previous attempts [25] used gamma retroviral vectors in a preclinical Rag1$^{-/-}$ model, which carried a high risk of insertional mutagenesis. Although RAG1 gamma retroviral vectors were able to correct the deficiency more readily, SIN lentiviral vectors initially resulted in insufficient expression of the therapeutic *RAG1* gene, leading to 'leaky' SCID or an Omenn-like phenotype. A breakthrough came with the introduction of codon-optimization of the human *RAG1* gene [26].This innovation yielded higher viral titers and much higher levels of *RAG1* expression without the need to introduce multiple copies per cell. Here we have used the same codon optimized *RAG1* therapeutic gene, but in a different lentiviral backbone and under the control of a clinically approved promoter. The first challenge was to develop a vector with a strong promoter driving the high expression of *c.o.RAG1*, to similar levels as native expression. According to Immgen dataset and our previous data in human thymi [40], native *Rag1* expression needed for B- and T-cell development in mouse is at least 10x and 13x the household gene expression (*Abl1*). In accordance, we here show that durable, functional immune reconstitution can be obtained at low VCN (1 or lower) with our MND-c.o.RAG1 vector that is consistently driving sufficient *c.o.RAG1* expression above 10x the household gene. As proper *RAG1*

expression was achieved, gene therapy treated mice survived healthy, without showing representative features of leaky SCID in mice as discussed by Marrella et al. (Rag2 Omenn syndrome mouse model [51]), Khiong et al. (Rag1 Omenn Syndrome [52]), Giblin et al. 2009 (Atypical SCID phenotype [53]) and Ott de Bruin et al. (CID-G/AI phenotype [54]). Our data suggest that the approach using pCCL-MND-c.o.RAG1 transduced HSCP should be able to overcome the broad range of clinical and immunologic phenotypes due to RAG1 deficiency, including hypomorphic RAG1 disease. Experimental proof for correction of hypomorphic RAG1 deficiencies requires extensive experimentation in appropriate mouse models, which are planned in the near future. Moreover, we show that the human RAG1 deficiency can be functionally restored in patient cells, providing important additional efficacy data required for successful clinical implementation.

In some mice, the reconstitution of T- and B-cell development with RAG1 transduced cells lagged behind compared to development observed in wild type stem cells. This indicates that some additional improvements could be made. For example, by optimizing transduction efficiencies which can be achieved by using a non-toxic transduction enhancer [55]; however, VCN numbers should not increase too much as this may increase insertional mutagenic events. Another approach to improve at least the T-cell development may be to co-transplant or the use of CD34+ CD7+ cells prior transplantation [56] [57] from the same patient to support the thymic microenvironment in which the stem/progenitor cells that seed the thymus find their niches. This can be especially important to boost development in the DN compartment.

Insertional mutagenesis has been shown to occur in gene therapy trials using γ-retroviral vectors without SIN configuration. In our study a SIN LV vector using the MND promoter was chosen, because this fairly strong promoter is most efficacious in our preclinical models. The MND promoter has previously been used in gene therapy trials for ADA-SCID [58] and Adrenoleukodystrophy (ALD), without any reports of insertional mutagenesis [59] [60]. In the ALD trials there were some clones showing clonal dominance with over-representation of insertion site near SMG6, CCND2 and HMGA2, but this has not led to development of leukemia and may be transient as was reported for a SIN LV vector used for treating β-thalassemia [61]. In addition, our collective preclinical safety data indicate that the MND-c.o.RAG1 vector is relatively safe. Nevertheless, genotoxicity cannot be fully excluded and we therefore favor clinical implementation initially in patients in whom only HLA incompatible donors are available. After clinical efficacy and safety has been demonstrated in this patient group, wider implementation could be considered; potentially, not only for RAG1-SCID, but also for Omenn Syndrome and other RAG1 deficiencies.

Clinical trials have shown that ADA-SCID and X-linked SCID gene therapies result in significant clinical benefit, as well as a significant reduction in healthcare-related costs (reviewed in [58] [62]). We expect similar benefits from our approach to treat patients with RAG1-SCID, as it will reduce the suboptimal outcomes in (mismatched) allogeneic transplants, which are often associated with the need to administer immunoglobulins, and treat infectious and GvHD-related complications. Based on the results reported here, a phase I/II clinical trial is planned to open in 2020. We expect that this trial will provide an

alternative curative treatment for patients with RAG1-SCID, for whom no matched stem cell donor is available.

SUPPLEMENTARY MATERIAL

A)

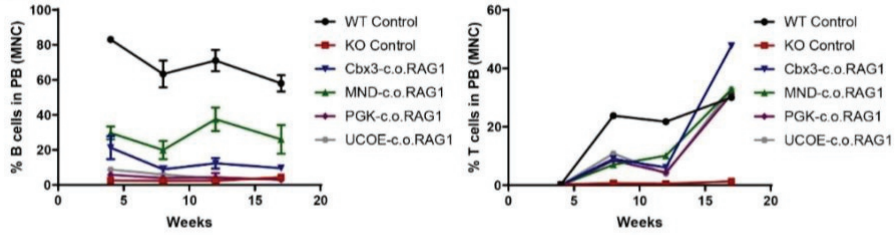

B)

In vitro	Cbx3-MND	MND	PGK	UCOE
Physical titer	++	++	+	+/-
Functional titer	+	++	+	+/-
Transgene expression	+	+	-	-
Promoter strength	++	+	-	+

C)

In vivo	Cbx3-MND	MND
B cell development BM	-	+
Thymic reconstitution	-	+
Mature immune cells	-	+
Immunoglobulins	-	+
T cell repertoire	+/-	+/-
Safety (IVIM)	+/-	+/-
Omenn-like syndrome in mice (due to low c.o.RAG1 expression)	Observed	Not observed

***Figure S1: Choice of the optimal SIN LV plasmid**. A) Percentage of B cells (CD11b/CD43-B220+ cells; left panel) and T cells (CD3+TCRαβ+ cells; right panel) over time in PB after stem cell transplantation with the different constructs (Cbx3.MND-c.o.RAG1, MND-c.o.RAG1, PGK-c.o.RAG1 and UCOE-c.o.RAG1) (Data from 2 independent experiments, total of 6-7 mice/group). B) Summary of the in vitro decision criteria (from 3 independent lentiviral batches) taken into account for the choice of the most optimal plasmid to correct RAG1 deficiency. C) Summary of the In vivo decision criteria (2 independent experiments with total of 6-7 mice per group) taken into account for the choice of the most optimal plasmid to correct RAG1 deficiency.*

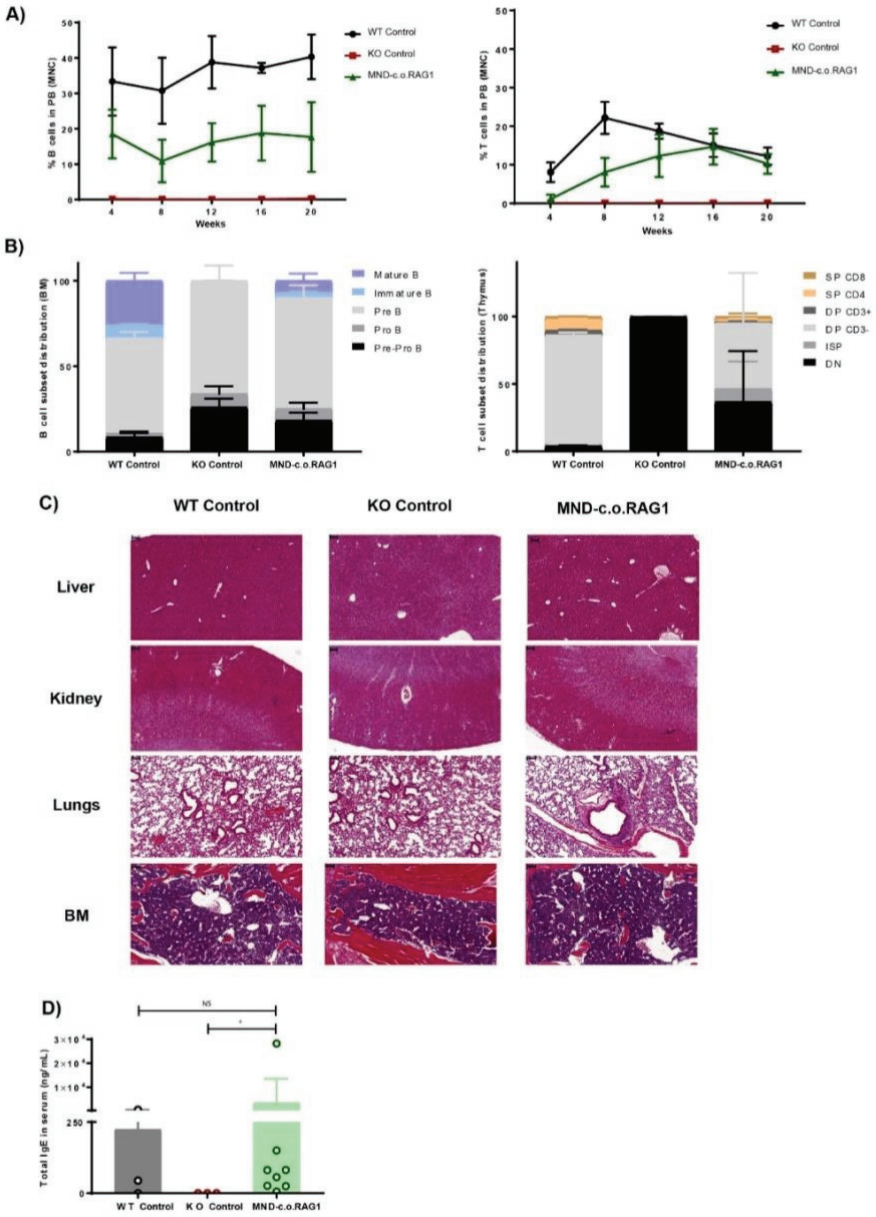

Figure S2: Immune development after MND-c.o.RAG1 gene therapy in Rag1-/- mouse model. *A) Percentage of B cells (CD11b/CD43-B220+ cells; left panel) and T cells (CD3+TCRαβ+ cells; right panel) over time in PB after stem cell transplantation with the clinical MND-c.o.RAG1 batch (3 WT control mice, 3 KO control mice and 8 MND-c.o.RAG1 mice). B) B-cell development subsets distribution in BM (left panel) and T-cell development populations distribution in the thymus (right panel) 24 weeks after SC transplantation. Graphs represent the means and standard deviation of 3 mice for control groups and 8 mice in the gene therapy group. C) Histologic analysis of the liver (scale bar = 100µm), kidney (scale bar=200µm), lungs (scale bar=100µm)* ***and BM*** *(scale=100µm) stained*

*with hematoxylin and eosin. Representative images from WT Control, KO Control and MND-c.o.RAG1 mice. D) Quantification of total IgE in serum by ELISA. Each dot represents a value obtained in one mouse (3 mice/control group, 8 MND-c.o.RAG1 mice). Mann-Whitney test (Two-tailed, *p<0,05; **p<0,01).*

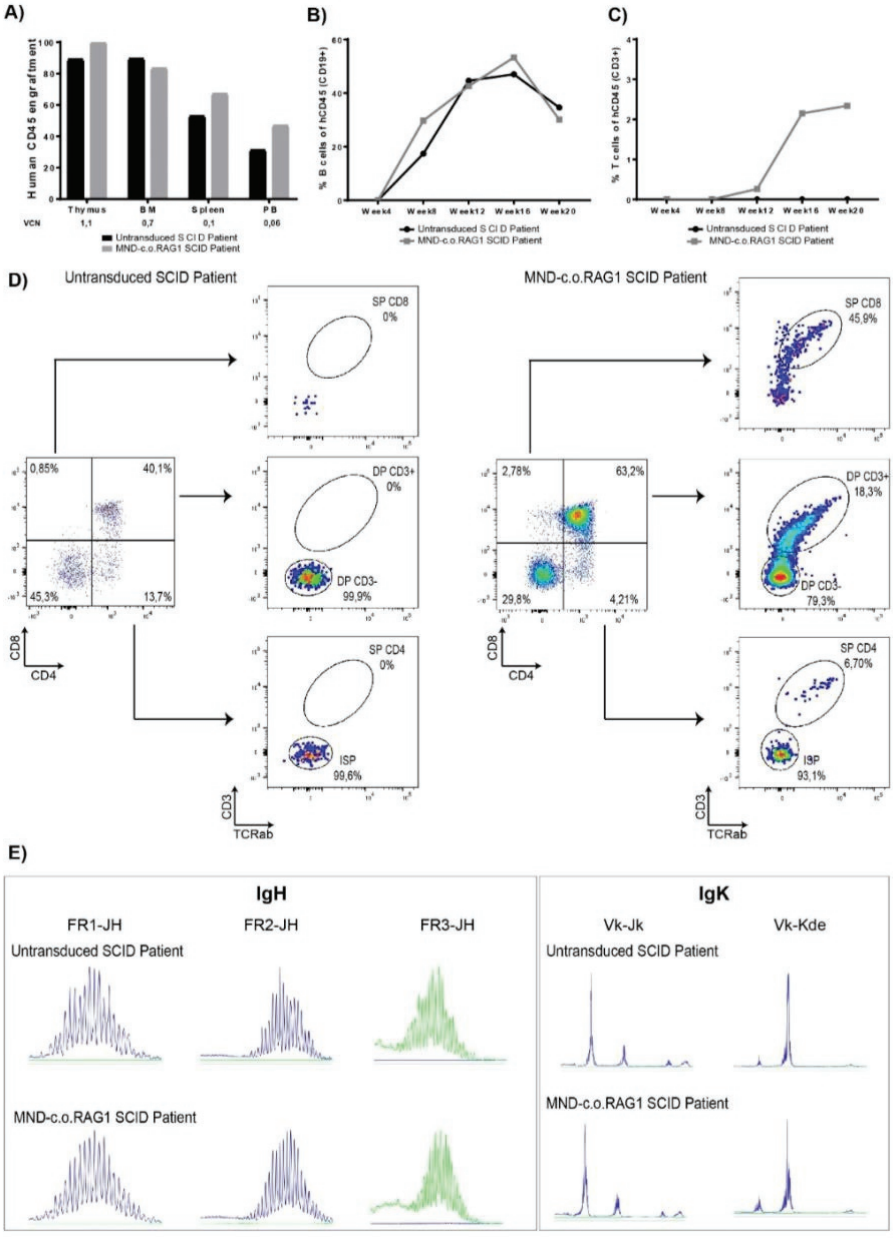

***Figure S3: Human immune reconstitution after CD34+ MND-c.o.RAG1 transplantation**. A) Percentage of human chimerism (hCD45+/(hCD45+mCD45+) in immune organs of NSG mice*

transplanted with CD34+ SCID patient cells and CD34+ SCID patient cells transduced with MND-c.o.RAG1, 24 weeks after transplantation (1 NSG mouse per condition). B) Human B-cell percentage (CD19+ cells per total hCD45+ cells) over time in peripheral blood during transplantation. C)Human T-cell development (CD3+ cells per total hCD45+ cells) over time in PB during transplantation. D) Flow cytometry analysis of thymocytes 24 weeks after transplantation showing T-cell development through the different stages. E) Human IgH and IgK repertoire analysis of isolated DNA from NSG BM (SCID patient and SCID MND-c.o.RAG1) using IgH + IgK B-Cell Clonality Assay. (x-axis indicates fragment sizes; y-axis shows the fluorescence intensity of the runoff products).

REFERENCES

1. Fischer, A.; Hacein-Bey-Abina, S.; Cavazzana-Calvo, M., 20 years of gene therapy for SCID. Nature immunology 2010, 11 (6), 457-60.

2. Griffith, L. M.; Cowan, M. J.; Notarangelo, L. D.; Puck, J. M.; Buckley, R. H.; Candotti, F.; Conley, M. E.; Fleisher, T. A.; Gaspar, H. B.; Kohn, D. B.; Ochs, H. D.; O'Reilly, R. J.; Rizzo, J. D.; Roifman, C. M.; Small, T. N.; Shearer, W. T., Improving cellular therapy for primary immune deficiency diseases: recognition, diagnosis, and management. The Journal of allergy and clinical immunology 2009, 124 (6), 1152-60 e12.

3. Grunebaum, E.; Mazzolari, E.; Porta, F.; Dallera, D.; Atkinson, A.; Reid, B.; Notarangelo, L. D.; Roifman, C. M., Bone marrow transplantation for severe combined immune deficiency. Jama 2006, 295 (5), 508-18.

4. Cavazzana-Calvo, M.; Fischer, A., Gene therapy for severe combined immunodeficiency: are we there yet? The Journal of clinical investigation 2007, 117 (6), 1456-65.

5. Gaspar, H. B.; Thrasher, A. J., Gene therapy for severe combined immunodeficiencies. Expert Opin Biol Ther 2005, 5 (9), 1175-82.

6. Noordzij, J. G.; de Bruin-Versteeg, S.; Verkaik, N. S.; Vossen, J. M.; de Groot, R.; Bernatowska, E.; Langerak, A. W.; van Gent, D. C.; van Dongen, J. J., The immunophenotypic and immunogenotypic B-cell differentiation arrest in bone marrow of RAG-deficient SCID patients corresponds to residual recombination activities of mutated RAG proteins. Blood 2002, 100 (6), 2145-52.

7. Romano, R.; Palamaro, L.; Fusco, A.; Iannace, L.; Maio, S.; Vigliano, I.; Giardino, G.; Pignata, C., From murine to human nude/SCID: the thymus, T-cell development and the missing link. Clinical & developmental immunology 2012, 2012, 467101.

8. Wiekmeijer, A. S.; Pike-Overzet, K.; Ijspeert, H.; Brugman, M. H.; Wolvers-Tettero, I. L.; Lankester, A.; Bredius, R. G.; Van Dongen, J. J.; Fibbe, W.; Langerak, A.; Van der Burg, M.; Staal, F. J., Identification of early checkpoints in human T-cell development using SCID stem cells. The Journal of allergy and clinical immunology 2015, in press.

9. Aiuti, A., Advances in gene therapy for ADA-deficient SCID. Curr Opin Mol Ther 2002, 4 (5), 515-22.

10. Aiuti, A.; Cassani, B.; Andolfi, G.; Mirolo, M.; Biasco, L.; Recchia, A.; Urbinati, F.; Valacca, C.; Scaramuzza, S.; Aker, M.; Slavin, S.; Cazzola, M.; Sartori, D.; Ambrosi, A.; Di Serio, C.; Roncarolo, M. G.; Mavilio, F.; Bordignon, C., Multilineage hematopoietic reconstitution without clonal selection in ADA-SCID patients treated with stem cell gene therapy. The Journal of clinical investigation 2007, 117 (8), 2233-40.

11. Aiuti, A.; Cattaneo, F.; Galimberti, S.; Benninghoff, U.; Cassani, B.; Callegaro, L.; Scaramuzza, S.; Andolfi, G.; Mirolo, M.; Brigida, I.; Tabucchi, A.; Carlucci, F.; Eibl, M.;

Aker, M.; Slavin, S.; Al-Mousa, H.; Al Ghonaium, A.; Ferster, A.; Duppenthaler, A.; Notarangelo, L.; Wintergerst, U.; Buckley, R. H.; Bregni, M.; Marktel, S.; Valsecchi, M. G.; Rossi, P.; Ciceri, F.; Miniero, R.; Bordignon, C.; Roncarolo, M. G., Gene therapy for immunodeficiency due to adenosine deaminase deficiency. The New England journal of medicine 2009, 360 (5), 447-58.

12. Carlucci, F.; Tabucchi, A.; Aiuti, A.; Rosi, F.; Floccari, F.; Pagani, R.; Marinello, E., Evaluation of ADA gene expression and transduction efficiency in ADA/SCID patients undergoing gene therapy. Nucleosides Nucleotides Nucleic Acids 2004, 23 (8-9), 1245-8.

13. Cavazzana-Calvo, M.; Hacein-Bey, S.; de Saint Basile, G.; Gross, F.; Yvon, E.; Nusbaum, P.; Selz, F.; Hue, C.; Certain, S.; Casanova, J. L.; Bousso, P.; Deist, F. L.; Fischer, A., Gene therapy of human severe combined immunodeficiency (SCID)-X1 disease. Science 2000, 288 (5466), 669-72.

14. Gaspar, H. B.; Parsley, K. L.; Howe, S.; King, D.; Gilmour, K. C.; Sinclair, J.; Brouns, G.; Schmidt, M.; Von Kalle, C.; Barington, T.; Jakobsen, M. A.; Christensen, H. O.; Al Ghonaium, A.; White, H. N.; Smith, J. L.; Levinsky, R. J.; Ali, R. R.; Kinnon, C.; Thrasher, A. J., Gene therapy of X-linked severe combined immunodeficiency by use of a pseudotyped gammaretroviral vector. Lancet 2004, 364 (9452), 2181-7.

15. Santilli, G.; Thornhill, S. I.; Kinnon, C.; Thrasher, A. J., Gene therapy of inherited immunodeficiencies. Expert Opin Biol Ther 2008, 8 (4), 397-407.

16. Hacein-Bey-Abina, S.; Von Kalle, C.; Schmidt, M.; McCormack, M. P.; Wulffraat, N.; Leboulch, P.; Lim, A.; Osborne, C. S.; Pawliuk, R.; Morillon, E.; Sorensen, R.; Forster, A.; Fraser, P.; Cohen, J. I.; de Saint Basile, G.; Alexander, I.; Wintergerst, U.; Frebourg, T.; Aurias, A.; Stoppa-Lyonnet, D.; Romana, S.; Radford-Weiss, I.; Gross, F.; Valensi, F.; Delabesse, E.; Macintyre, E.; Sigaux, F.; Soulier, J.; Leiva, L. E.; Wissler, M.; Prinz, C.; Rabbitts, T. H.; Le Deist, F.; Fischer, A.; Cavazzana-Calvo, M., LMO2-associated clonal T cell proliferation in two patients after gene therapy for SCID-X1. Science 2003, 302 (5644), 415-9.

17. Kohn, D. B.; Sadelain, M.; Glorioso, J. C., Occurrence of leukaemia following gene therapy of X-linked SCID. Nature reviews. Cancer 2003, 3 (7), 477-88.

18. Pike-Overzet, K.; de Ridder, D.; Weerkamp, F.; Baert, M. R.; Verstegen, M. M.; Brugman, M. H.; Howe, S. J.; Reinders, M. J.; Thrasher, A. J.; Wagemaker, G.; van Dongen, J. J.; Staal, F. J., Gene therapy: is IL2RG oncogenic in T-cell development? Nature 2006, 443 (7109), E5; discussion E6-7.

19. Pike-Overzet, K.; van der Burg, M.; Wagemaker, G.; van Dongen, J. J.; Staal, F. J., New insights and unresolved issues regarding insertional mutagenesis in X-linked SCID gene therapy. Mol Ther 2007, 15 (11), 1910-6.

20. Howe, S. J.; Mansour, M. R.; Schwarzwaelder, K.; Bartholomae, C.; Hubank, M.; Kempski, H.; Brugman, M. H.; Pike-Overzet, K.; Chatters, S. J.; de Ridder, D.; Gilmour, K. C.; Adams, S.; Thornhill, S. I.; Parsley, K. L.; Staal, F. J.; Gale, R. E.; Linch, D. C.; Bayford, J.; Brown, L.; Quaye, M.; Kinnon, C.; Ancliff, P.; Webb, D. K.; Schmidt, M.; von Kalle, C.; Gaspar, H. B.; Thrasher, A. J., Insertional mutagenesis combined with acquired somatic mutations causes leukemogenesis following gene therapy of SCID-X1 patients. The Journal of clinical investigation 2008, 118 (9), 3143-50.

21. Montini, E.; Cesana, D.; Schmidt, M.; Sanvito, F.; Bartholomae, C. C.; Ranzani, M.; Benedicenti, F.; Sergi, L. S.; Ambrosi, A.; Ponzoni, M.; Doglioni, C.; Di Serio, C.; von Kalle, C.; Naldini, L., The genotoxic potential of retroviral vectors is strongly modulated by vector design and integration site selection in a mouse model of HSC gene therapy. The Journal of clinical investigation 2009, 119 (4), 964-75.

22. Thornhill, S. I.; Schambach, A.; Howe, S. J.; Ulaganathan, M.; Grassman, E.; Williams, D.; Schiedlmeier, B.; Sebire, N. J.; Gaspar, H. B.; Kinnon, C.; Baum, C.; Thrasher, A. J., Self-inactivating gammaretroviral vectors for gene therapy of X-linked severe combined immunodeficiency. Molecular therapy : the journal of the American Society of Gene Therapy 2008, 16 (3), 590-8.

23. Benjelloun, F.; Garrigue, A.; Demerens-de Chappedelaine, C.; Soulas-Sprauel, P.; Malassis-Seris, M.; Stockholm, D.; Hauer, J.; Blondeau, J.; Riviere, J.; Lim, A.; Le Lorc'h, M.; Romana, S.; Brousse, N.; Paques, F.; Galy, A.; Charneau, P.; Fischer, A.; de Villartay, J. P.; Cavazzana-Calvo, M., Stable and functional lymphoid reconstitution in artemis-deficient mice following lentiviral artemis gene transfer into hematopoietic stem cells. Molecular therapy : the journal of the American Society of Gene Therapy 2008, 16 (8), 1490-9.

24. Lagresle-Peyrou, C.; Yates, F.; Malassis-Seris, M.; Hue, C.; Morillon, E.; Garrigue, A.; Liu, A.; Hajdari, P.; Stockholm, D.; Danos, O.; Lemercier, B.; Gougeon, M. L.; Rieux-Laucat, F.; de Villartay, J. P.; Fischer, A.; Cavazzana-Calvo, M., Long-term immune reconstitution in RAG-1-deficient mice treated by retroviral gene therapy: a balance between efficiency and toxicity. Blood 2006, 107 (1), 63-72.

25. Lagresle-Peyrou, C.; Benjelloun, F.; Hue, C.; Andre-Schmutz, I.; Bonhomme, D.; Forveille, M.; Beldjord, K.; Hacein-Bey-Abina, S.; De Villartay, J. P.; Charneau, P.; Durandy, A.; Fischer, A.; Cavazzana-Calvo, M., Restoration of human B-cell differentiation into NOD-SCID mice engrafted with gene-corrected CD34+ cells isolated from Artemis or RAG1-deficient patients. Molecular therapy : the journal of the American Society of Gene Therapy 2008, 16 (2), 396-403.

26. Pike-Overzet, K.; Rodijk, M.; Ng, Y. Y.; Baert, M. R.; Lagresle-Peyrou, C.; Schambach, A.; Zhang, F.; Hoeben, R. C.; Hacein-Bey-Abina, S.; Lankester, A. C.; Bredius, R. G.; Driessen, G. J.; Thrasher, A. J.; Baum, C.; Cavazzana-Calvo, M.; van Dongen, J. J.; Staal, F. J., Correction of murine Rag1 deficiency by self-inactivating lentiviral vector-mediated gene transfer. Leukemia 2011, 25 (9), 1471-83.

27. van Til, N. P.; Sarwari, R.; Visser, T. P.; Hauer, J.; Lagresle-Peyrou, C.; van der Velden, G.; Malshetty, V.; Cortes, P.; Jollet, A.; Danos, O.; Cassani, B.; Zhang, F.; Thrasher, A. J.; Fontana, E.; Poliani, P. L.; Cavazzana, M.; Verstegen, M. M. A.; Villa, A.; Wagemaker, G., Recombination-activating gene 1 (Rag1)–deficient mice with severe combined immunodeficiency treated with lentiviral gene therapy demonstrate autoimmune Omenn-like syndrome. Journal of Allergy and Clinical Immunology 2014, 133 (4), 1116-1123.

28. Pike-Overzet, K.; Baum, C.; Bredius, R. G.; Cavazzana, M.; Driessen, G. J.; Fibbe, W. E.; Gaspar, H. B.; Hoeben, R. C.; Lagresle-Peyrou, C.; Lankester, A.; Meij, P.; Schambach, A.; Thrasher, A.; Van Dongen, J. J.; Zwaginga, J. J.; Staal, F. J., Successful RAG1-SCID gene therapy depends on the level of RAG1 expression. J Allergy Clin Immunol 2014, 134 (1), 242-3.

29. Baum, C.; Kustikova, O.; Modlich, U.; Li, Z.; Fehse, B., Mutagenesis and oncogenesis by chromosomal insertion of gene transfer vectors. Hum Gene Ther 2006, 17 (3), 253-63.

30. Dull, T.; Zufferey, R.; Kelly, M.; Mandel, R. J.; Nguyen, M.; Trono, D.; Naldini, L., A third-generation lentivirus vector with a conditional packaging system. J Virol 1998, 72 (11), 8463-71.

31. Pannetier, C.; Cochet, M.; Darche, S.; Casrouge, A.; Zöller, M.; Kourilsky, P., The sizes of the CDR3 hypervariable regions of the murine T-cell receptor beta chains vary as a function of the recombined germ-line segments. Proceedings of the National Academy of Sciences of the United States of America 1993, 90 (9), 4319-4323.

32. Cordes, M.; Pike-Overzet, K.; van Eggermond, M.; Vloemans, S.; Baert, M. R.; Garcia-Perez, L.; Staal, F. J. T.; Reinders, M. J. T.; van den Akker, E., ImSpectR - R package to

quantify immune repertoire diversity in spectratype and repertoire sequencing data. Bioinformatics 2019.

33. van Dongen, J. J. M.; Langerak, A. W.; Brüggemann, M.; Evans, P. A. S.; Hummel, M.; Lavender, F. L.; Delabesse, E.; Davi, F.; Schuuring, E.; García-Sanz, R.; van Krieken, J. H. J. M.; Droese, J.; González, D.; Bastard, C.; White, H. E.; Spaargaren, M.; González, M.; Parreira, A.; Smith, J. L.; Morgan, G. J.; Kneba, M.; Macintyre, E. A., Design and standardization of PCR primers and protocols for detection of clonal immunoglobulin and T-cell receptor gene recombinations in suspect lymphoproliferations: Report of the BIOMED-2 Concerted Action BMH4-CT98-3936. Leukemia 2003, 17, 2257.

34. Gabriel, R.; Kutschera, I.; Bartholomae, C. C.; von Kalle, C.; Schmidt, M., Linear amplification mediated PCR--localization of genetic elements and characterization of unknown flanking DNA. J Vis Exp 2014, (88), e51543.

35. Modlich, U.; Bohne, J.; Schmidt, M.; von Kalle, C.; Knöss, S.; Schambach, A.; Baum, C., Cell-culture assays reveal the importance of retroviral vector design for insertional genotoxicity. Blood 2006, 108 (8), 2545-2553.

36. WHO, WHO guidelines on nonclinical evaluation of vaccines. Organization, W. H., Ed. Tech Rep Ser, 2005; pp 31-63.

37. Bancroft, J. D.; Gamble, M., Theory and Practice of Histological Techniques. Churchill Livingstone: 2008.

38. Halene, S.; Wang, L.; Cooper, R. M.; Bockstoce, D. C.; Robbins, P. B.; Kohn, D. B., Improved expression in hematopoietic and lymphoid cells in mice after transplantation of bone marrow transduced with a modified retroviral vector. Blood 1999, 94 (10), 3349-57.

39. Knight, S.; Zhang, F.; Mueller-Kuller, U.; Bokhoven, M.; Gupta, A.; Broughton, T.; Sha, S.; Antoniou, M. N.; Brendel, C.; Grez, M.; Thrasher, A. J.; Collins, M.; Takeuchi, Y., Safer, silencing-resistant lentiviral vectors: optimization of the ubiquitous chromatin-opening element through elimination of aberrant splicing. J Virol 2012, 86 (17), 9088-95.

40. Dik, W. A.; Pike-Overzet, K.; Weerkamp, F.; de Ridder, D.; de Haas, E. F.; Baert, M. R.; van der Spek, P.; Koster, E. E.; Reinders, M. J.; van Dongen, J. J.; Langerak, A. W.; Staal, F. J., New insights on human T cell development by quantitative T cell receptor gene rearrangement studies and gene expression profiling. The Journal of experimental medicine 2005, 201 (11), 1715-23.

41. Pike-Overzet, K.; Rodijk, M.; Ng, Y. Y.; Baert, M. R. M.; Lagresle-Peyrou, C.; Schambach, A.; Zhang, F.; Hoeben, R. C.; Hacein-Bey-Abina, S.; Lankester, A. C.; Bredius, R. G. M.; Driessen, G. J. A.; Thrasher, A. J.; Baum, C.; Cavazzana-Calvo, M.; van Dongen, J. J. M.; Staal, F. J. T., Correction of murine Rag1 deficiency by self-inactivating lentiviral vector-mediated gene transfer. Leukemia 2011, 25, 1471.

42. Wiekmeijer, A. S.; Pike-Overzet, K.; Brugman, M. H.; Salvatori, D. C.; Egeler, R. M.; Bredius, R. G.; Fibbe, W. E.; Staal, F. J., Sustained Engraftment of Cryopreserved Human Bone Marrow CD34(+) Cells in Young Adult NSG Mice. BioResearch open access 2014, 3 (3), 110-6.

43. Wiekmeijer, A. S.; Pike-Overzet, K.; H, I. J.; Brugman, M. H.; Wolvers-Tettero, I. L.; Lankester, A. C.; Bredius, R. G.; van Dongen, J. J.; Fibbe, W. E.; Langerak, A. W.; van der Burg, M.; Staal, F. J., Identification of checkpoints in human T-cell development using severe combined immunodeficiency stem cells. The Journal of allergy and clinical immunology 2016, 137 (2), 517-526 e3.

44. Gennery, A. R.; Slatter, M. A.; Grandin, L.; Taupin, P.; Cant, A. J.; Veys, P.; Amrolia, P. J.; Gaspar, H. B.; Davies, E. G.; Friedrich, W.; Hoenig, M.; Notarangelo, L. D.;

Mazzolari, E.; Porta, F.; Bredius, R. G.; Lankester, A. C.; Wulffraat, N. M.; Seger, R.; Gungor, T.; Fasth, A.; Sedlacek, P.; Neven, B.; Blanche, S.; Fischer, A.; Cavazzana-Calvo, M.; Landais, P., Transplantation of hematopoietic stem cells and long-term survival for primary immunodeficiencies in Europe: entering a new century, do we do better? The Journal of allergy and clinical immunology 126 (3), 602-10 e1-11.

45. Haddad, E.; Logan, B. R.; Griffith, L. M.; Buckley, R. H.; Parrott, R. E.; Prockop, S. E.; Small, T. N.; Chaisson, J.; Dvorak, C. C.; Murnane, M.; Kapoor, N.; Abdel-Azim, H.; Hanson, I. C.; Martinez, C.; Bleesing, J. J. H.; Chandra, S.; Smith, A. R.; Cavanaugh, M. E.; Jyonouchi, S.; Sullivan, K. E.; Burroughs, L.; Skoda-Smith, S.; Haight, A. E.; Tumlin, A. G.; Quigg, T. C.; Taylor, C.; Davila Saldana, B. J.; Keller, M. D.; Seroogy, C. M.; Desantes, K. B.; Petrovic, A.; Leiding, J. W.; Shyr, D. C.; Decaluwe, H.; Teira, P.; Gillio, A. P.; Knutsen, A. P.; Moore, T. B.; Kletzel, M.; Craddock, J. A.; Aquino, V.; Davis, J. H.; Yu, L. C.; Cuvelier, G. D. E.; Bednarski, J. J.; Goldman, F. D.; Kang, E. M.; Shereck, E.; Porteus, M. H.; Connelly, J. A.; Fleisher, T. A.; Malech, H. L.; Shearer, W. T.; Szabolcs, P.; Thakar, M. S.; Vander Lugt, M. T.; Heimall, J.; Yin, Z.; Pulsipher, M. A.; Pai, S. Y.; Kohn, D. B.; Puck, J. M.; Cowan, M. J.; O'Reilly, R. J.; Notarangelo, L. D., SCID genotype and 6-month posttransplant CD4 count predict survival and immune recovery. Blood 2018, 132 (17), 1737-1749.

46. De Ravin, S. S.; Wu, X.; Moir, S.; Anaya-O'Brien, S.; Kwatemaa, N.; Littel, P.; Theobald, N.; Choi, U.; Su, L.; Marquesen, M.; Hilligoss, D.; Lee, J.; Buckner, C. M.; Zarember, K. A.; O'Connor, G.; McVicar, D.; Kuhns, D.; Throm, R. E.; Zhou, S.; Notarangelo, L. D.; Hanson, I. C.; Cowan, M. J.; Kang, E.; Hadigan, C.; Meagher, M.; Gray, J. T.; Sorrentino, B. P.; Malech, H. L.; Kardava, L., Lentiviral hematopoietic stem cell gene therapy for X-linked severe combined immunodeficiency. Science translational medicine 2016, 8 (335), 335ra57.

47. Touzot, F.; Moshous, D.; Creidy, R.; Neven, B.; Frange, P.; Cros, G.; Caccavelli, L.; Blondeau, J.; Magnani, A.; Luby, J. M.; Ternaux, B.; Picard, C.; Blanche, S.; Fischer, A.; Hacein-Bey-Abina, S.; Cavazzana, M., Faster T-cell development following gene therapy compared with haploidentical HSCT in the treatment of SCID-X1. Blood 2015, 125 (23), 3563-9.

48. Cavazzana, M.; Six, E.; Lagresle-Peyrou, C.; Andre-Schmutz, I.; Hacein-Bey-Abina, S., Gene Therapy for X-Linked Severe Combined Immunodeficiency: Where Do We Stand? Hum Gene Ther 2016, 27 (2), 108-16.

49. Mortellaro, A.; Hernandez, R. J.; Guerrini, M. M.; Carlucci, F.; Tabucchi, A.; Ponzoni, M.; Sanvito, F.; Doglioni, C.; Di Serio, C.; Biasco, L.; Follenzi, A.; Naldini, L.; Bordignon, C.; Roncarolo, M. G.; Aiuti, A., Ex vivo gene therapy with lentiviral vectors rescues adenosine deaminase (ADA)-deficient mice and corrects their immune and metabolic defects. Blood 2006, 108 (9), 2979-88.

50. Kohn, D. B.; Kuo, C. Y., New frontiers in the therapy of primary immunodeficiency: From gene addition to gene editing. Journal of Allergy and Clinical Immunology 2017, 139 (3), 726-732.

51. Marrella, V.; Poliani, P. L.; Casati, A.; Rucci, F.; Frascoli, L.; Gougeon, M. L.; Lemercier, B.; Bosticardo, M.; Ravanini, M.; Battaglia, M.; Roncarolo, M. G.; Cavazzana-Calvo, M.; Facchetti, F.; Notarangelo, L. D.; Vezzoni, P.; Grassi, F.; Villa, A., A hypomorphic R229Q Rag2 mouse mutant recapitulates human Omenn syndrome. The Journal of clinical investigation 2007, 117 (5), 1260-9.

52. Khiong, K.; Murakami, M.; Kitabayashi, C.; Ueda, N.; Sawa, S.; Sakamoto, A.; Kotzin, B. L.; Rozzo, S. J.; Ishihara, K.; Verella-Garcia, M.; Kappler, J.; Marrack, P.; Hirano, T., Homeostatically proliferating CD4 T cells are involved in the pathogenesis of an Omenn syndrome murine model. The Journal of clinical investigation 2007, 117 (5), 1270-81.

53. Giblin, W.; Chatterji, M.; Westfield, G.; Masud, T.; Theisen, B.; Cheng, H. L.; DeVido, J.; Alt, F. W.; Ferguson, D. O.; Schatz, D. G.; Sekiguchi, J., Leaky severe combined immunodeficiency and aberrant DNA rearrangements due to a hypomorphic RAG1 mutation. Blood 2009, 113 (13), 2965-75.

54. Ott de Bruin, L. M.; Bosticardo, M.; Barbieri, A.; Lin, S. G.; Rowe, J. H.; Poliani, P. L.; Ching, K.; Eriksson, D.; Landegren, N.; Kampe, O.; Manis, J. P.; Notarangelo, L. D., Hypomorphic Rag1 mutations alter the preimmune repertoire at early stages of lymphoid development. Blood 2018, 132 (3), 281-292.

55. Delville, M.; Soheili, T.; Bellier, F.; Durand, A.; Denis, A.; Lagresle-Peyrou, C.; Cavazzana, M.; Andre-Schmutz, I.; Six, E., A Nontoxic Transduction Enhancer Enables Highly Efficient Lentiviral Transduction of Primary Murine T Cells and Hematopoietic Stem Cells. Molecular therapy. Methods & clinical development 2018, 10, 341-347.

56. Six, E. M.; Benjelloun, F.; Garrigue, A.; Bonhomme, D.; Morillon, E.; Rouiller, J.; Cacavelli, L.; Blondeau, J.; Beldjord, K.; Hacein-Bey-Abina, S.; Cavazzana-Calvo, M.; Andre-Schmutz, I., Cytokines and culture medium have a major impact on human in vitro T-cell differentiation. Blood Cells Mol Dis 2011, 47 (1), 72-8.

57. Reimann, C.; Six, E.; Dal-Cortivo, L.; Schiavo, A.; Appourchaux, K.; Lagresle-Peyrou, C.; de Chappedelaine, C.; Ternaux, B.; Coulombel, L.; Beldjord, K.; Cavazzana-Calvo, M.; Andre-Schmutz, I., Human T-lymphoid progenitors generated in a feeder-cell-free Delta-like-4 culture system promote T-cell reconstitution in NOD/SCID/gammac(-/-) mice. Stem cells 2012, 30 (8), 1771-80.

58. Morgan, R. A.; Gray, D.; Lomova, A.; Kohn, D. B., Hematopoietic Stem Cell Gene Therapy: Progress and Lessons Learned. Cell Stem Cell 2017, 21 (5), 574-590.

59. Eichler, F.; Duncan, C.; Musolino, P. L.; Orchard, P. J.; De Oliveira, S.; Thrasher, A. J.; Armant, M.; Dansereau, C.; Lund, T. C.; Miller, W. P.; Raymond, G. V.; Sankar, R.; Shah, A. J.; Sevin, C.; Gaspar, H. B.; Gissen, P.; Amartino, H.; Bratkovic, D.; Smith, N. J. C.; Paker, A. M.; Shamir, E.; O'Meara, T.; Davidson, D.; Aubourg, P.; Williams, D. A., Hematopoietic Stem-Cell Gene Therapy for Cerebral Adrenoleukodystrophy. New England Journal of Medicine 2017, 377 (17), 1630-1638.

60. Cartier, N.; Hacein-Bey-Abina, S.; Bartholomae, C. C.; Veres, G.; Schmidt, M.; Kutschera, I.; Vidaud, M.; Abel, U.; Dal-Cortivo, L.; Caccavelli, L.; Mahlaoui, N.; Kiermer, V.; Mittelstaedt, D.; Bellesme, C.; Lahlou, N.; Lefrere, F.; Blanche, S.; Audit, M.; Payen, E.; Leboulch, P.; l'Homme, B.; Bougneres, P.; Von Kalle, C.; Fischer, A.; Cavazzana-Calvo, M.; Aubourg, P., Hematopoietic stem cell gene therapy with a lentiviral vector in X-linked adrenoleukodystrophy. Science 2009, 326 (5954), 818-23.

61. Cavazzana-Calvo, M.; Payen, E.; Negre, O.; Wang, G.; Hehir, K.; Fusil, F.; Down, J.; Denaro, M.; Brady, T.; Westerman, K.; Cavallesco, R.; Gillet-Legrand, B.; Caccavelli, L.; Sgarra, R.; Maouche-Chretien, L.; Bernaudin, F.; Girot, R.; Dorazio, R.; Mulder, G. J.; Polack, A.; Bank, A.; Soulier, J.; Larghero, J.; Kabbara, N.; Dalle, B.; Gourmel, B.; Socie, G.; Chretien, S.; Cartier, N.; Aubourg, P.; Fischer, A.; Cornetta, K.; Galacteros, F.; Beuzard, Y.; Gluckman, E.; Bushman, F.; Hacein-Bey-Abina, S.; Leboulch, P., Transfusion independence and HMGA2 activation after gene therapy of human beta-thalassaemia. Nature 2010, 467 (7313), 318-22.

62. Staal, F. J. T.; Aiuti, A.; Cavazzana, M., Autologous Stem-Cell-Based Gene Therapy for Inherited Disorders: State of the Art and Perspectives. Frontiers in Pediatrics 2019, 7 (443).